U.S. Department
of Transportation
**Federal Railroad
Administration**

Stub Sills on Tank Cars

Final Report

W. J. Walsh
R. C. Rice
D. R. Ahlbeck

BATTELLE
Columbus Division
505 King Avenue
Columbus, Ohio 43201-2693

**Office of Research
and Development**
DOT/FRA/ORD-89/01

March 1989

This document is available for purchase from the National Technical Information Service, U.S. Department of Commerce, Springfield, VA 22161

NOTICE

The United States Government does not endorse products or manufacturers. Trade or manufacturers' names appear herein solely because they are considered essential to the object of this report.

NOTICE

This document is disseminated under the sponsorship of the Department of Transportation in the interest of information exchange. The United States Government assumes no liability for its contents or use thereof.

Technical Report Documentation Page

1. Report No.	2. Government Accession No.	3. Recipient's Catalog No.
FRA/ORD-89-01		

4. Title and Subtitle	5. Report Date
Stub Sills on Tank Cars	March 1989
	6. Performing Organization Code
	8. Performing Organization Report No.
7. Author(s)	
W. J. Walsh, R. C. Rice, D. R. Ahlbeck	
9. Performing Organization Name and Address Battelle 505 King Avenue Columbus OH 43201-2693	10. Work Unit No. (TRAIS)
	11. Contract or Grant No. DTFR53-86-C-00006
	13. Type of Report and Period Covered Final Report
12. Sponsoring Agency Name and Address U.S. Department of Transportation Federal Railraod Administration Office of Research and Development Washington, D.C. 20590	14. Sponsoring Agency Code RRS-32

15. Supplementary Notes

16. Abstract

The results of this study indicate that the head brace repair procedure provides an effective means for redirecting stub sill loads into the tank body. thus reducing stresses at the critical sill-to-reinforcing pad weld sites. Our analysis indicates that the stub sill to tank interface stresses from longitudinal coupler loads are reduced significantly (by about 15 to 20 percent) and the stresses due to vertical coupler loads are reduced dramatically (by over 75 percent). The longitudinal coupler loads are most influential in terms of crack initiation, while the vertical coupler loads were found to influence crack growth to a greater extent.

Therefore, it has been concluded that the stub sill designs, with the head brace properly installed, will exhibit significantly longer service lives before fatigue cracks form (if they form at all). Perhaps even more importantly, the introduction of the head brace should offer an important margin of safety in terms of crack growth life. In other words, even if fatigue cracks do form at the stub sill to tank interface and the head brace is intact, crack growth rates should be reduced to such an extent that the likelihood of properly identifying and repairing these cracks before tank rupture should be increased significantly. If the head brace itself cracks, the damage should be relatively easy to identify and repair.

In summary, the introduction of a properly sized and installed head brace should offer an effective means of reducing the likelihood of both fatigue crack initiation and tank rupture. However, the procedure does not eliminate the need for periodic inspection of the region for fatigue damage.

17. Key Words	18. Distribution Statement
Stub Sills, Tank Cars, Stress Analysis, Fatigue, Life Prediction, Head Brace	Document is available to the public the National Technical Information Service, Springfield, VA 22161

19. Security Classif. (of this report)	20. Security Classif. (of this page)	21. No. of Pages	22. Price
Unclassified	Unclassified	60	

METRIC CONVERSION FACTORS

Approximate Conversions to Metric Measures

Symbol	When You Know	Multiply by	To Find	Symbol
LENGTH				
in	inches	*2.5	centimeters	cm
ft	feet	30	centimeters	cm
yd	yards	0.9	meters	m
mi	miles	1.6	kilometers	km
AREA				
in^2	square inches	6.5	square centimeters	cm^2
ft^2	square feet	0.09	square meters	m^2
yd^2	square yards	0.8	square meters	m^2
mi^2	square miles	2.6	square kilometers	km^2
	acres	0.4	hectares	ha
MASS (weight)				
oz	ounces	28	grams	g
lb	pounds	0.45	kilograms	kg
	short tons (2000 lb)	0.9	tonnes	t
VOLUME				
tsp	teaspoons	5	milliliters	ml
Tbsp	tablespoons	15	milliliters	ml
fl oz	fluid ounces	30	milliliters	ml
c	cups	0.24	liters	l
pt	pints	0.47	liters	l
qt	quarts	0.95	liters	l
gal	gallons	3.8	liters	l
ft^3	cubic feet	0.03	cubic meters	m^3
yd^3	cubic yards	0.76	cubic meters	m^3
TEMPERATURE (exact)				
°F	Fahrenheit temperature	5/9 (after subtracting 32)	Celsius temperature	°C

*1 in. = 2.54 cm (exactly). For other exact conversions and more detail tables see NBS Misc. Publ. 286, Units of Weight and Measures. Price $2.25 SD Catalog No. C13 10 286.

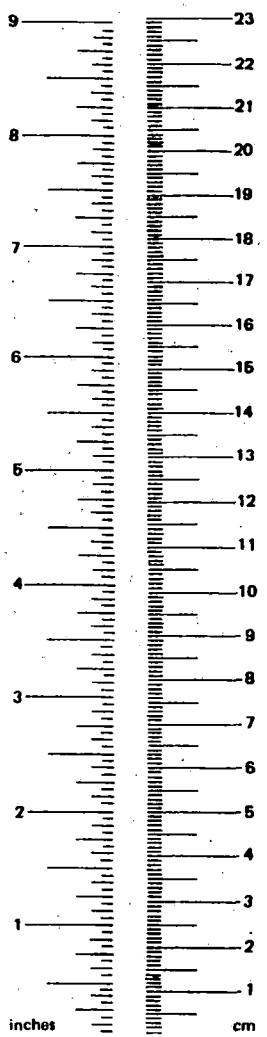

Approximate Conversions from Metric Measures

Symbol	When You Know	Multiply by	To Find	Symbol
LENGTH				
mm	millimeters	0.04	inches	in
cm	centimeters	0.4	inches	in
m	meters	3.3	feet	ft
m	meters	1.1	yards	yd
km	kilometers	0.6	miles	mi
AREA				
cm^2	square centimeters	0.16	square inches	in^2
m^2	square meters	1.2	square yards	yd^2
km^2	square kilometers	0.4	square miles	mi^2
ha	hectares (10,000 m^2)	2.5	acres	
MASS (weight)				
g	grams	0.035	ounces	oz
kg	kilograms	2.2	pounds	lb
t	tonnes (1000 kg)	1.1	short tons	
VOLUME				
ml	milliliters	0.03	fluid ounces	fl oz
l	liters	2.1	pints	pt
l	liters	1.06	quarts	qt
l	liters	0.26	gallons	gal
m^3	cubic meters	36	cubic feet	ft^3
m^3	cubic meters	1.3	cubic yards	yd^3
TEMPERATURE (exact)				
°C	Celsius temperature	9/5 (then add 32)	Fahrenheit temperature	°F

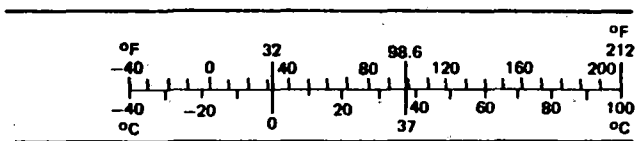

TABLE OF CONTENTS

LIST OF TABLES

LIST OF FIGURES

SUMMARY

This task was initiated in February of 1987. The objective for Battelle was to evaluate the safety of the design of stub sill tank cars presently experiencing cracks and the safety of repairs being made.

This final report summarizes the results of the following tasks:

- Survey and Problem Definition
- Loads Definition
- Stress Analysis
- Fatigue Life Estimation
- Analysis of Stub Sill Repairs
- Evaluation of Accuracy and Sources of Uncertainty.

The results of this study indicate that the head brace concept is an effective repair procedure for redirecting stub sill loads into the tank body, thus reducing stresses at the critical sill-to-reinforcing pad weld. The head brace repair procedure is used for Richmond and North American type tank cars. Our analysis indicates that the stub sill to tank interface stresses from longitudinal coupler loads have been reduced significantly (by about 15 to 20 percent) and the stresses due to vertical coupler loads have been reduced dramatically (by over 75 percent). The longitudinal coupler loads appear to be most influential in terms of crack initiation, while the vertical coupler loads may influence crack growth to a greater extent.

Therefore, it is logical to conclude that stub sill designs, with the head brace properly installed, will exhibit longer service lives before fatigue cracks form (if they form at all). Perhaps even more importantly, introduction of the head brace should offer an important margin of safety in terms of crack growth life. In other words, even if fatigue cracks do form at the stub sill to tank interface and the head brace is intact, crack growth rates should be reduced to such an extent that the likelihood of properly identifying and repairing these cracks before tank rupture will be increased significantly. If the head brace itself cracks, the damage should be relatively easy to identify and repair.

In summary, introduction of a properly sized and installed head brace does offer an effective means of reducing the likelihood of both

fatigue crack initiation and tank rupture, but the procedure does not eliminate the need for periodic inspection of the region for fatigue damage.

INTRODUCTION

Over the past several years, tank cars in DOT Classes 105A, 111A, 112A, 112S, and 112T that are stub sill designs, have experienced cracking at the stub sill/tank car interface. On some cars, the cracks extend to the bottom of both sides of the stub sill. When cracks are found, they are repaired.

On February 4, 1985, a stub sill tank car released anhydrous hydrogen fluoride due to a crack in an undercut weld at the tank car head. The National Transportation Safety Board (NTSB) investigated the hazardous material release and concluded that the head to stub sill weld attachment was a critical stress area. The NTSB believes that this area requires frequent and intensive inspections and monitoring to detect potential failures. The NTSB recommended that the Federal Railroad Administration (FRA) "develop a recertification program for tank cars in hazardous materials service fabricated prior to 1967, which will provide assurance that undercut welds in tank car heads are identified and corrected."

The problems that have developed at the inboard and outboard ends of the reinforcing pad used for the stub sill attachment have involved cracks due to fatigue, buckling leading to cracks, and welding quality problems. These three factors singly or in combination have been responsible for one of the most frequently recurring problems on tank cars. The accident investigated by the NTSB was considered to be a final indication of the need for a detailed review of the stub sill tank car attachment.

As a result, the FRA's Office of Research and Development initiated this special task, instructing Battelle to evaluate the safety of the design of stub sill tank cars presently experiencing cracks and the safety of repairs being made.

SURVEY AND PROBLEM DEFINITION

In order to define and understand the extent of the stub sill cracking problem, a series of trips and phone conversations was completed. First, the FRA offices in Washington, D.C., were visited to collect background information. A collection of photographs, drawings and reports were obtained pertaining to the stub sill cracking problem. The Department of Transportation's Transportation Systems Center (DOT/TSC) was also visited to discuss the tank car fatigue and fracture work underway there.

Subsequently, contacts were established with all of the major tank car companies. Mr. Earl Phillips was visited at the Association of American Railroads (AAR) in Chicago to arrange a meeting of the Railway Progress Institute's (RPI) Tank Car Technical and Engineering (TCT&E) Subcommittee. (Mr. Phillips is the Program Manager of the RPI-AAR Railroad Tank Car Safety Research and Test Project and, in that capacity serves as an interface between the tank car companies and outside parties.)

A meeting with the RPI TCT&E Subcommittee was held to explain the goals of the FRA task and to define the industry's position on the cause and extent of the problem. Messrs. R. C. Rice, W. J. Walsh and M. J. Rosenfeld participated for Battelle. The representatives for each of the tank car companies were as follows:

Mr. B. J. Damiani Vice President Engineering	Union Tank Car Company
Mr. W. L. Finn Vice President, Fleet Operations	ACF Industries, Inc.
Mr. E. Mowatt-Larssen Director--Technical Engineering	General American Tank Car Company
Mr. R. A. Boerke Manager, Engineering	GE Rail Car Services
Mr. S. Smith Manager, Engineering	Trinity Industries

Also in attendance were Mr. Phillips and Mr. L. Olsen, representing the AAR.

The unanimous feeling among the tank car manufacturers was that the reported accidents were simply isolated incidents resulting from poor welds. They did not feel that there was an inherent design problem with any specific stub sill tank car design, or with tank cars in general.

This initial meeting was followed the next day by visits to the individual car manufacturers in the Chicago area. Union Tank Car Company in East Chicago and GE Rail Car Services agreed to visits. Stub sill tank car drawings were provided Battelle at both Union Tank Car and GE Rail Car. Mr. Boerke of GE Rail Car summarized the cracking problems experienced by the North American tank cars in the GE fleet by saying that cracks generally initiate at the sill to pad weld.

A third car manufacturer, ACF Industries in St. Louis, was also visited. ACF engineers agreed to provide drawings of their dual diameter tank cars which were experiencing cracks. They also agreed to provide information on the frequency and type of repairs performed on these cars during a recent repair program.

Richmond Industries in Houston was also contacted, specifically in connection with the BCDX 498 accident (described below). Mr. P. Hayes, Director of Engineering, agreed to send drawings of cars in the ECUX 575000 series. He also informed Battelle that Richmond and Exxon had performed a joint study of the cracking problem experienced by Richmond-built cars. The program involved laboratory testing and fatigue life estimates for the cars, both before and after the present repair procedure (installation of a head brace). The report was submitted to the AAR in June, 1987. A copy was sent to Battelle the following month.

As a result of the survey activities described above, Battelle identified the following stub sill tank car cracking incidents.

(1) BCDX 498 (ECUX 575000 type), built by Richmond Tank Car Company, was found leaking in Seattle, Washington, April 4, 1985. The crack originated at the sill-to-pad weld.

(Refer to Figure 1.) Exxon Chemical Americas Company has 175 cars of a similar construction to BCDX 498. It is known that at least 41 of these cars were inspected at the G.E. repair plant in Texarkana, Arkansas. Thirteen of these cars were found to have cracked reinforcing pads; one had cracks at both ends. Those cars found to have cracks were repaired by removal of the original weld, rewelding, and application of a head brace fitted between the sill and reinforcing pad.

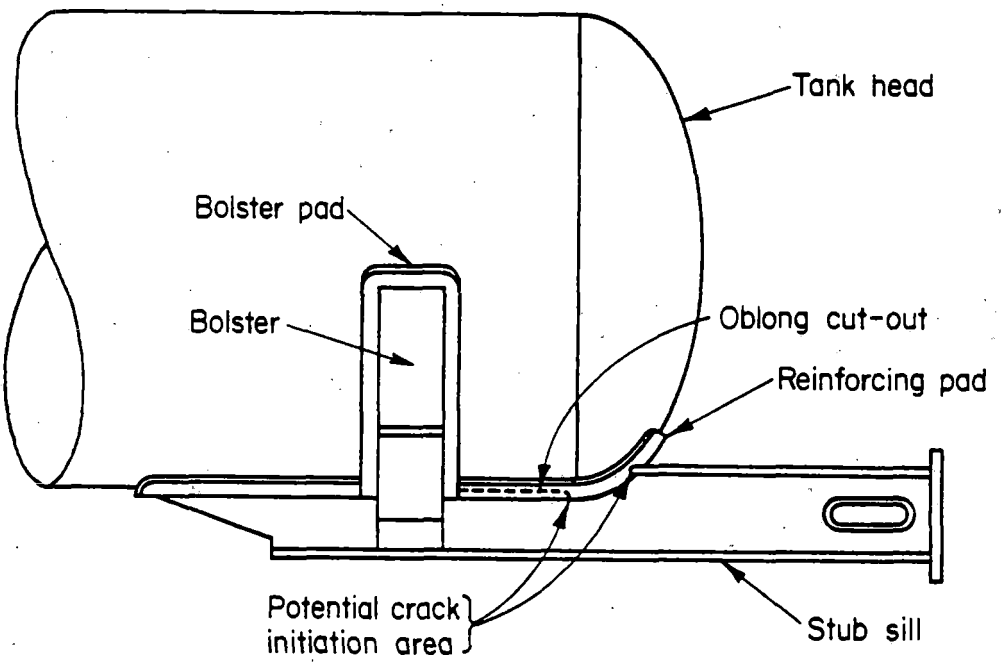

FIGURE 1. RICHMOND TYPE CAR

(2) ACF dual diameter design tank cars fabricated between 1962 and 1969; these cars are of two design types called long overhang and short overhang. Cracking has occurred in the cradle pad-to-tank weld in the short overhang cars. (Refer to Figure 2.) The cars have been inspected and repaired. These cars have not been involved in leak incidents to Battelle's knowledge.

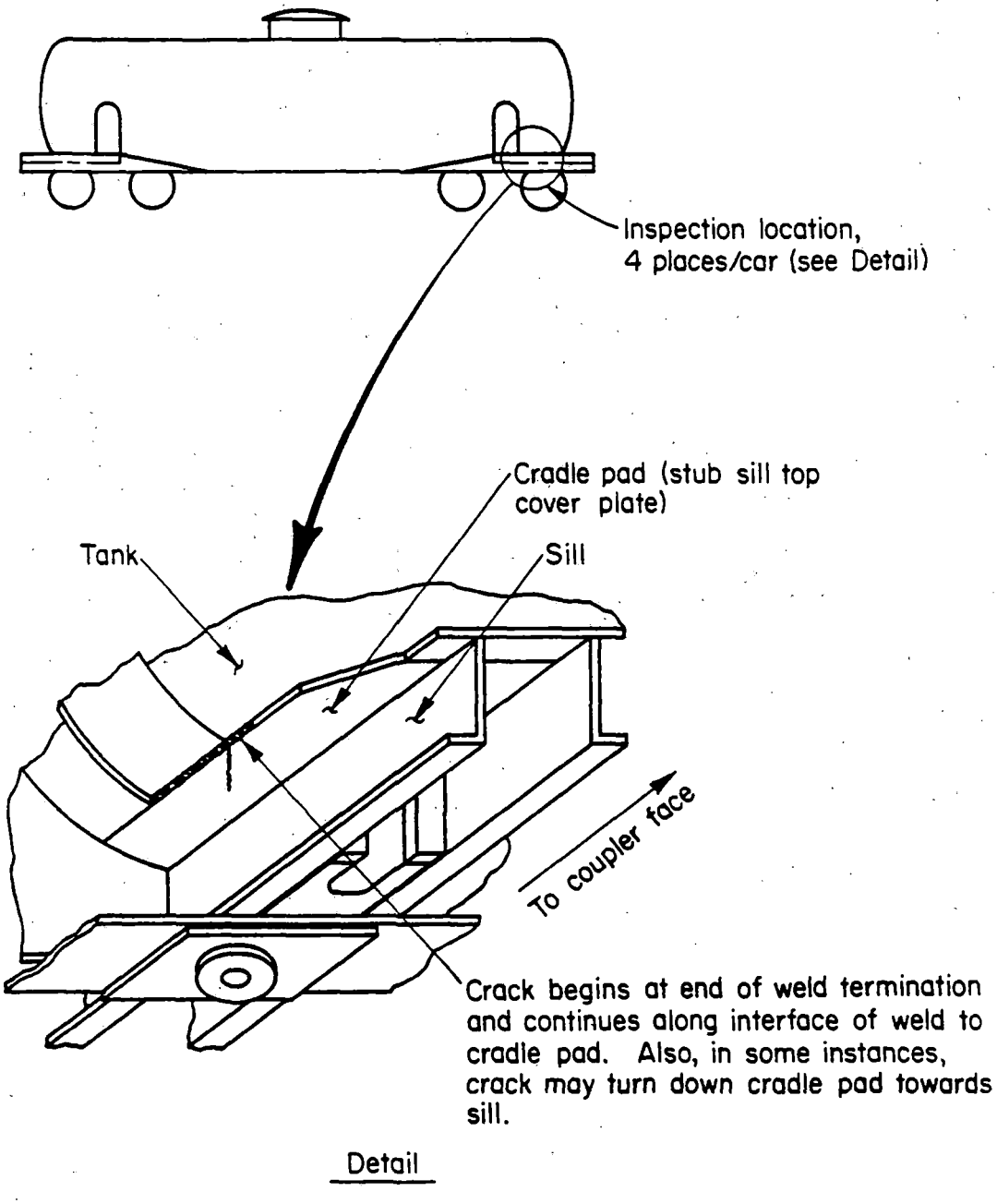

FIGURE 2. ACF INDUSTRIES FABRICATED STUB SILL TANK CAR INSPECTION INFORMATION

(3) NATX 34081 of the G.E. Railcar Services fleet was found leaking in Elkhart, Indiana on February 4, 1985. The crack originated at the sill-to-pad weld as shown in Figure 3. Since that occurrence, G.E. routinely modifies cars of this design by welding a head brace between the reinforcing pad and the sill, as shown in Figure 4, regardless of whether cracks are found.

(4) OCCX 1001 was found leaking in Pasadena, Texas on April 9, 1986. The weld joining the stub sill to the tank head at both the A and B ends had fractured.

(5) GATX 98862 was found leaking in a Beaumont, Texas shipping yard on November 9, 1984. A crack developed at the reinforcing pad-to-tank weld.

(6) GATX 98859 was found leaking in Hamlet, North Carolina on May 2, 1987. As with the GATX 98862 incident, a crack formed at the reinforcing pad-to-tank interface.

(7) NATX 13657 was found leaking in a shipping yard in Campbellton, New Brunswick, Canada on January 4, 1986. The crack occurred as a result of a patch welded on the tank near the sill.

Of the incidents cited, Number 7 appears to be an isolated incident. Only one case of this type of cracking has been identified. Numbers 1-6 however, appear to be recurring problems warranting further investigation. The cars involved in incident Numbers 3 and 4, NATX 34081 and OCCX 1001 have superficially similar designs based upon photographs of these cars included in FRA memoranda.

The GATX 988--series has had three leaking incidents reported* regarding cracks occurring at the reinforcement pad-to-tank interface, as shown in Figure 5. The similarity in cracking mode suggests that

---

* One of these incidents involved an HCPX 1713 built by GATX. It was found leaking at Baltimore, Maryland on February 28, 1986. A crack formed at the reinforcing pad-to-tank interface. Data for this car were not available for this analysis.

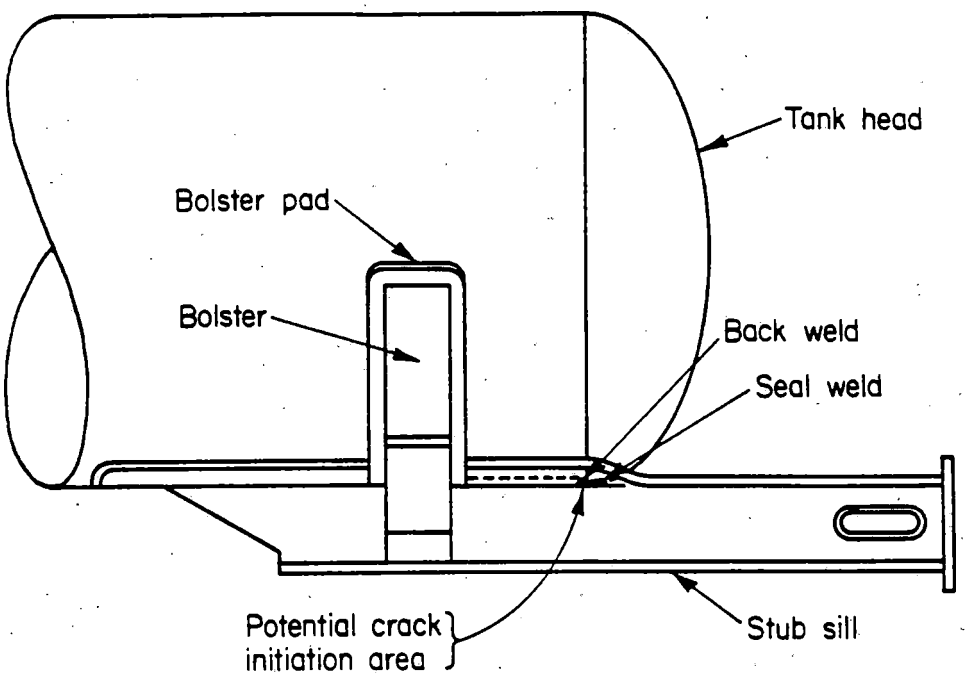

FIGURE 3. NORTH AMERICAN TYPE CAR

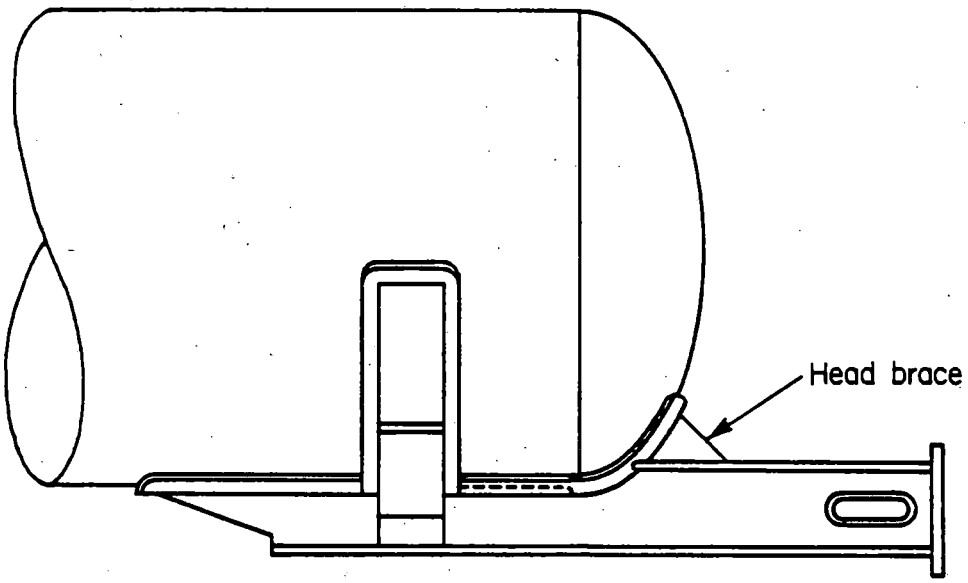

FIGURE 4. HEAD BRACE ARRANGEMENT

there might be a problem with the GATX head brace design. The GATX head brace has a vertical front face welded perpendicular to the sill. The reinforcing pad is also considerably smaller than those used by other tank car manufacturers. The GATX head brace reinforcing pad is 14-inches wide by 12-inches long. By comparison, the reinforcing pad in other head brace designs is generally 18-inches wide and extends below the sill. The smaller size of the pad and the mode of cracking suggest that perhaps too much of the load is transferred through this reinforcement pad to the tank.

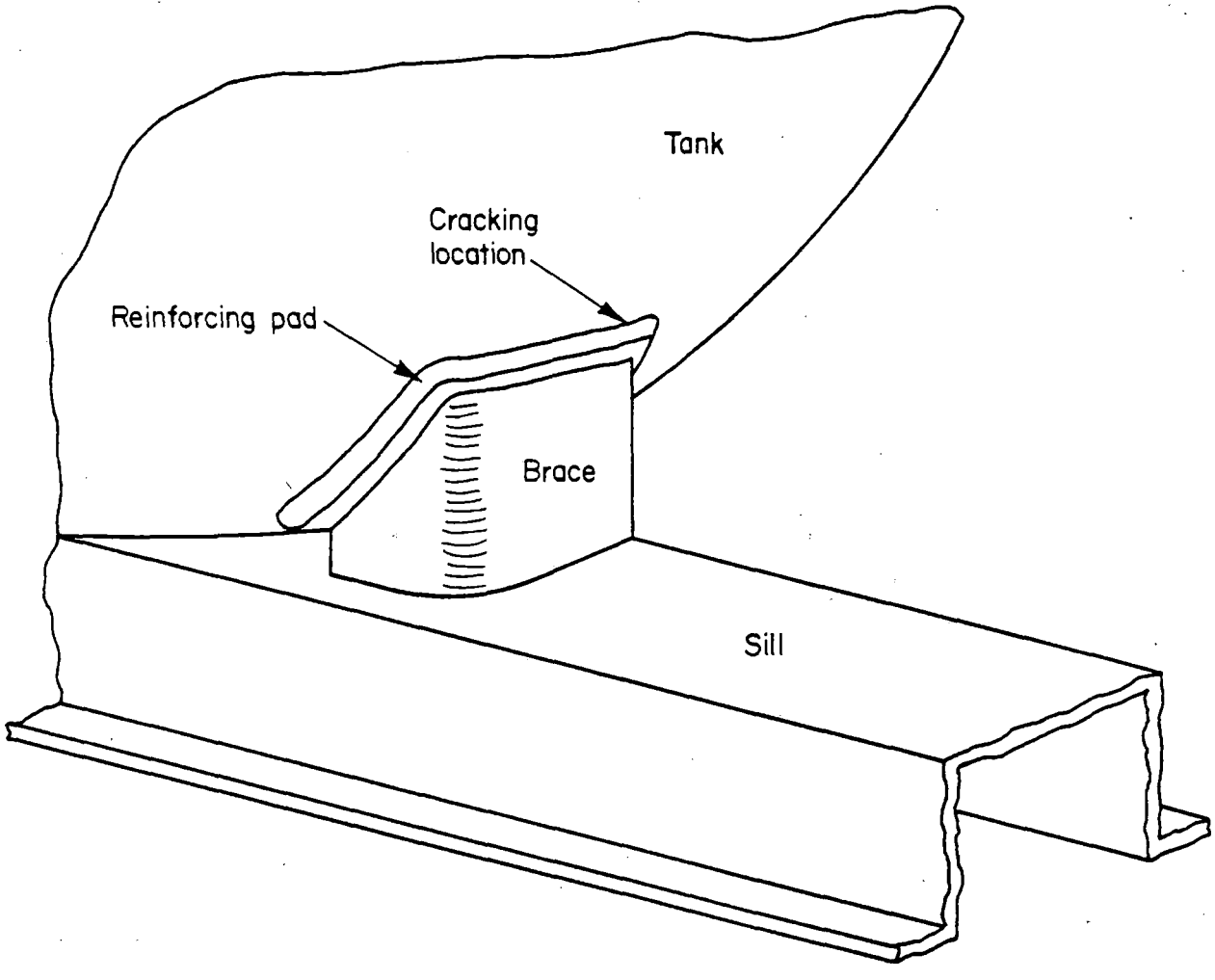

FIGURE 5. LOCATION OF LEAKING INCIDENTS WITH HEAD-BRACE MODIFIED GATX 988 SERIES TANK CARS

In summary, four designs have been identified as having potential for repeated cracking problems. These are:

(1) Richmond Tank Car ECUX 575000 series, DOT specification 105A300W. The 105A400W cars were also found to have some cracks upon inspection.
(2) ACF dual diameter tank cars
(3) North American Tank Cars, NATX 34081 type.
(4) GATX cars with the original vertical head brace installed.

ANALYSIS PROCEDURE

The objective of this study was to evaluate the potential for cracking at the stub sill/tank interface and evaluate the proposed repair procedures. The analyses consisted of finite element stress analyses of the tank cars in their as-built and repaired condition to determine the reduction in stress at the critical cracking location. Also, a loads definition activity was performed to characterize the load spectrum that a tank car would typically experience. Fatigue life estimates were performed using weldment fatigue estimation techniques.

The original plan was to develop finite element models and perform fatigue life predictions for each tank car design separately because of differences in the sill-to-tank interface geometries. This proved to be too ambitious an undertaking for the scope of this study. As an alternative, the decision was made to evaluate the head brace design concept as a repair procedure for Designs 1, 3, and 4.

Since the ACF dual diameter design (Design 2), was significantly different from the other three designs it was necessary to analyze this design separately. In this case the sill-to-pad interface developed cracks along a longitudinal weld joining the cradle pad and the tank. (The other designs cracked transverse to the sill.) As such, a head brace repair procedure was not appropriate for the ACF dual diameter design. Rather, stiffening wing bars were welded on the sill

to resist the sill flexure thought to be responsible for the cracking. This repair procedure has been implemented on all of the 1300 dual diameter cars in the ACF fleet. Since the ACF cars have not been involved in a leaking incident (to the best of our knowledge), this design was to be analyzed last if funds permitted. A finite element model was constructed from ACF dual diameter tank car drawings. However, as the study progressed it became apparent that funds would not be sufficient to perform the stress and fatigue analyses on this design. Therefore, complete stress and fatigue analyses were performed only for design types (1), (3) and (4).

Loads Definition

Railroad freight car shock and vibration can be characterized in two distinct categories: that occurring from over-the-road travel, and that occurring during classification (switching) of cars. Over-the-road loads and accelerations consist (at the car body) of a relatively low-level random vibration on which repetitive transients are superimposed from sources such as rail joints and wheel flats. Occasional higher-level transient shock pulses occur from traversing switch points and frogs, railroad crossings (diamonds), roadway grade crossings, as well as longitudinal impacts due to run-in and run-out of coupler slack from train-action dynamics. Shock pulses during classification yard operations (hump or flat-yard switching) result from longitudinal impacts when cars are coupled at speeds ranging typically from about 4 to 8 mph, but occasionally higher. Shock response spectra, which can be used to estimate peak accelerations of cargo in response to a transient event, are generally an order-of-magnitude higher in frequency content for switching events than for over-the road events.

Load and acceleration levels in response to the environment result from a combination of the rail vehicle and track characteristics, and train speed. Few peak accelerations greater than 1 g at the car body occur during over-the-road operations, and continuous vibration levels are relatively low during operations on good track. Sustained

high-amplitude vibrations and repetitive shock inputs can occur, however, due to low-frequency harmonic excitation from track geometry variations or due to car body or truck hunting instabilities.

Appendix A includes a synopsis of pertinent references regarding the load environment on 100 ton cars. The following paragraphs are based on these data, along with other information. They provide a summary of Battelle's best estimate of the loading environment on typical stub sill tank cars.

The use of bolted 39-foot rails with half-staggered joints results in a car roll excitation, particularly if the truck center distance is close to the rail length. Loaded freight cars will exhibit a roll resonant speed typically between 15 and 22 mph (0.56 to 0.83 Hz on 39-foot rail). If the track geometry is severe enough (low joints), the car will rock onto the side bearings and exceed the total spring travel, producing high side bearing loads. Computer simulations of 100-ton car rocking by Battelle[1]* have shown that the centerplate edge forces range from 130 to 160 thousand pounds (kips) (for a static vertical load of 120 kips), and side bearing forces range from 80 to 150 kips. Similarly, computer simulations by the AAR[2] have predicted maximum centerplate loads of 179 kips, and side bearing forces up to 186 kips. Other investigators such as T. Willis of IITRI[3] and Pullman-Standard[4] have predicted similar load levels at the side bearings and centerplate.

Tests by the Canadian National[5], the AAR[6], and Dresser Industries[7] on 100-ton hopper cars confirmed these predicted loads. The AAR tests on a covered hopper car produced measured centerplate vertical loads up to 170 kips, side bearing loads up to 158 kips, as well as lateral loads from bolster to side frame up to 20 kips. Tests by IITRI[8] resulted in measured side bearing loads up to 130 kips. Shock loads of 140 kips or higher are transmitted to the centerplate under these conditions as the car rocks from one side bearing to the

---

* References listed on page 49. See also Appendix A where a synopsis of references regarding the load environment on 100-ton cars is provided.

other, lifting off the centerplate twice during each roll cycle. The the 100-ton tank car, however, showed less tendency toward car rocking than the 100-ton open-top hopper car in these tests.

The most severe condition encountered with the tank car occurred on rough, bolted-joint track in the 45-60 mph speed range, where the car experienced a combined bounce/high-center roll oscillation. (The severe oscillation may have been partially due to the fact that the propane tank cars were filled about half full of water for the experiment.) Maximum measured loads on the centerplate ("truck bounce" loads) of 360 kips, an acceleration of 3 g, were measured about once every 4 miles under these conditions. In this extreme case, the track geometry-induced response drove the springs solid. It is also likely that occasional surface geometry errors at grade crossings and turnouts would also induce vertical bounce sufficient to bottom the springs. These loads would be carried through the centerplate into the car structure. Later tests by IITRI[9] on better-maintained track and on the FAST track at the Transportation Test Center (TTC) showed (as one might expect) a much lower vertical load exceedence curve, as shown in Figure 6.

A final and rather difficult step in the vertical centerplate load definition was to establish a reasonable composite load environment that included the effects of varied operations. Track conditions, for example, may vary significantly from railroad to railroad (or from division to division), and change with time between maintenance cycles, with seasonal climatic conditions, or as economic conditions change. These track conditions affect primarily the vertical load spectrum at the centerplate and the vertical loads with Type-F couplers. (The specific F coupler design used for this study was not identified in Reference 9.)

To account for these variations, some estimate of mileage accumulated under these different conditions had to be made. For this study, a composite load curve of vertical (bounce) loads, into the loaded tank car body was developed from the three load exceedance curves

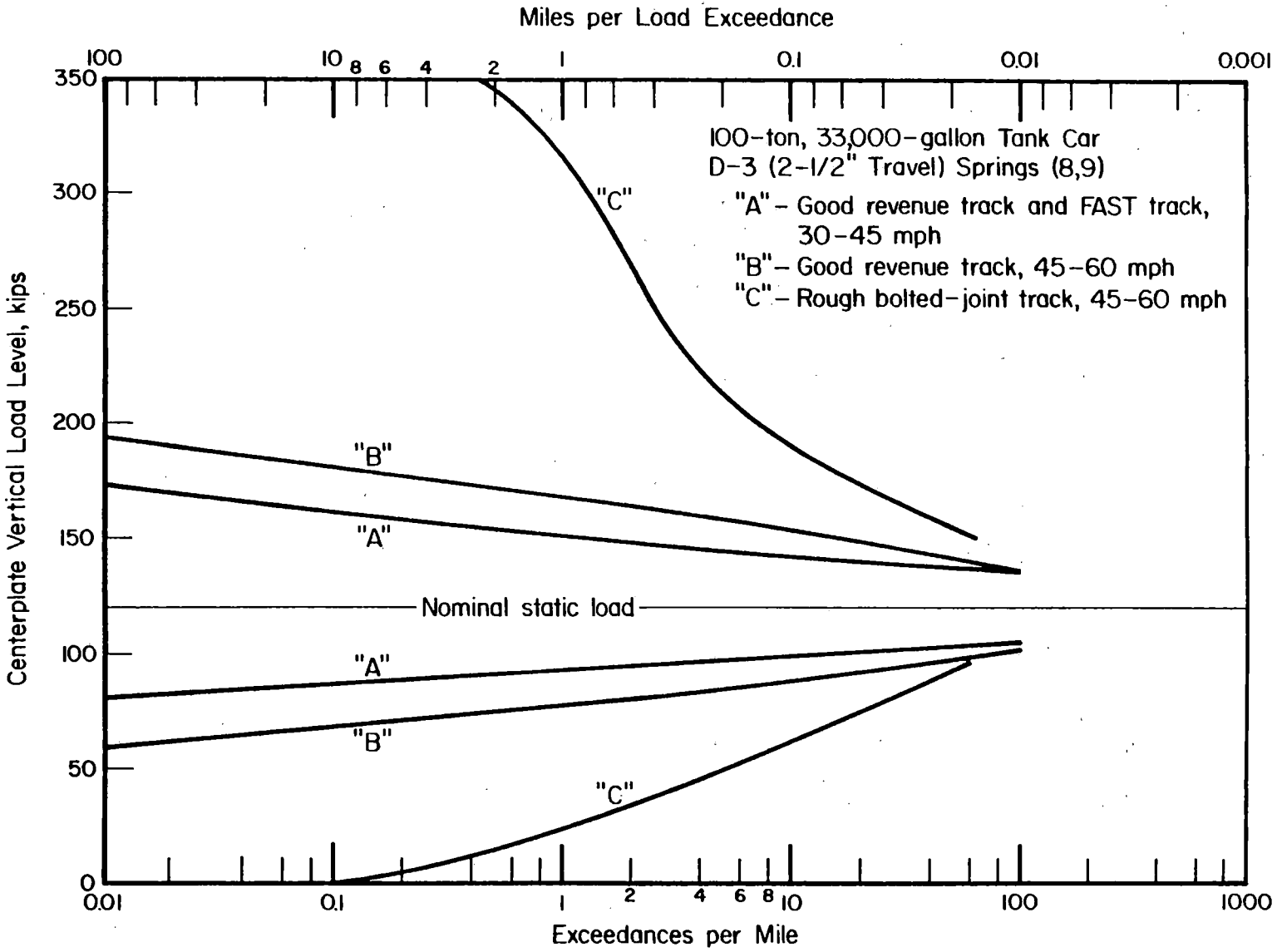

FIGURE 6. RANGE OF VERTICAL LOAD ENVIRONMENT AT CENTERPLATE OF 100-TON LOADED TANK CAR

of Figure 6. The following mileage weighting was used as shown in Figure 7.

Curve A: Good revenue track, 30-45 mph--45%
Curve B: Good revenue track, 45-60 mph--50%
Curve C: Rough bolted-joint track, 45-60 mph--5%

This weighting covers the loaded-car mileage only, roughly one-half the total tank car miles. Empty-car vertical loads are assumed to be modest by comparison, with centerplate peak loads under 50,000 lb. even on rough bolted-joint track.

In over-the-road operation, the vertical axis predominates as the load axis with the highest shock and vibration levels. High shock response has been noted in the lateral axis, however, due to truck hunting with empty or lightly loaded cars. Impact loads due to periodic flange contact can produce lateral accelerations of 1 g or greater on the car body during severe hunting. Hunting occurs at a frequency of 2 to 3.5 Hz, but the resulting impact loads have broader-band frequency content that can excite structural resonances.

Typical maximum longitudinal forces[10] of 250 kips in draft (3 SD50 locomotives in Notch 8 at 15 mph) and 150 kips in buff (maximum dynamic braking at 30 mph) have been measured. Tests by Freightmaster[11] on coupler run-in and run-out forces in over-the-road operations showed peak loads ranging up to 430 kips in buff and 345 kips in draft. Again, the frequency content of run-in and run-out impact loads is broad-band due to the stiffness of the draft gear.

Shock spectra for switching impacts show the longitudinal axis to be the most severe below about 10 Hz, while the vertical axis is most severe at higher frequencies. With a conventional draft gear (the type expected to be used with a tank car), an 8 mph coupling impact would produce a dynamic input varying from about +8 to -4 g on a loaded 50-ton car, which translates to a peak load of about 1000 kips, with a full-sine duration of about 50 milliseconds. The car body will then respond in the vertical axis due to the offset center of mass, exciting body

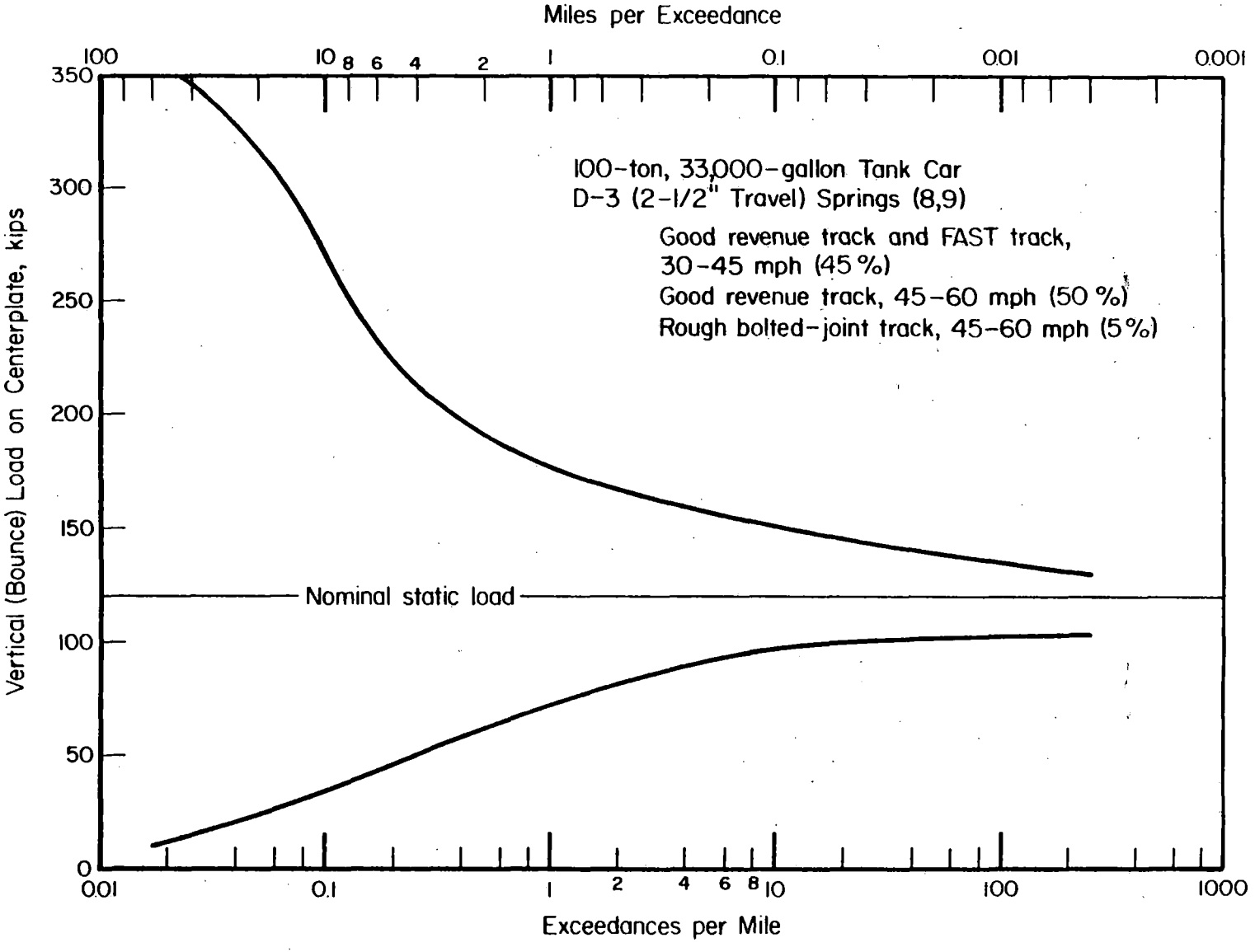

FIGURE 7. COMPOSITE LOAD EXCEEDANCE CURVES FOR VERTICAL LOADS INTO TANK CAR BODY, PER TRUCK -- LOADED-CAR MILEAGE

bending natural frequencies. With an empty tank car, these bending frequencies have been calculated to be 40 Hz or higher. Tests by IITRI[12] (with an empty 100-ton hopper car impacting three loaded "anvil" cars with brakes on, coupler-slack-bunched), showed the standard draft gear to bottom out at 6-7 mph impact speed. The peak buff load was found to rise rapidly from about 300 kips to nearly 1200 kips at 9.2 mph, with a half-sine load pulse of 27-milliseconds in duration. In a survey by Battelle of transportation shock and vibration environments[13], yard coupling speed distributions were determined, as summarized below.

Coupling Speed (mph)	Events (%)
< 6	70
6-7	17
7-8	7
8-9	3
9-10	2
> 10	1

A more recent study by Sandia[14] Laboratories showed that 99.8 percent of coupling impacts are less than or equal to 11 mph. Tests conducted by du Pont[15] on bulkhead flatcars carrying heavy nuclear casks showed high longitudinal loads into the couplers. Impacts at speeds between 10.5 and 11.2 mph produced measured loads up to 1620 kips. Recent tests conducted by the AAR[16] under the Freight Equipment Environmental Sampling Test (FEEST) program to determine over-the-road coupler loads, including some yard impact events, resulted in the load exceedance diagrams shown in Figure 8. Additional impact loading data became available from the Richmond Tank Car Company report titled "Evaluation of the Draft Sill to Tank Interface on Pressure Cars"[17]. The data consists of a coupler force vs. input speed plot and a histogram for impact speed. The source of the data was only identified as a "major car builder". The data shown in Figures 9 and 10, suggest that about 2 percent of all coupler loads exceed 1700 kips.

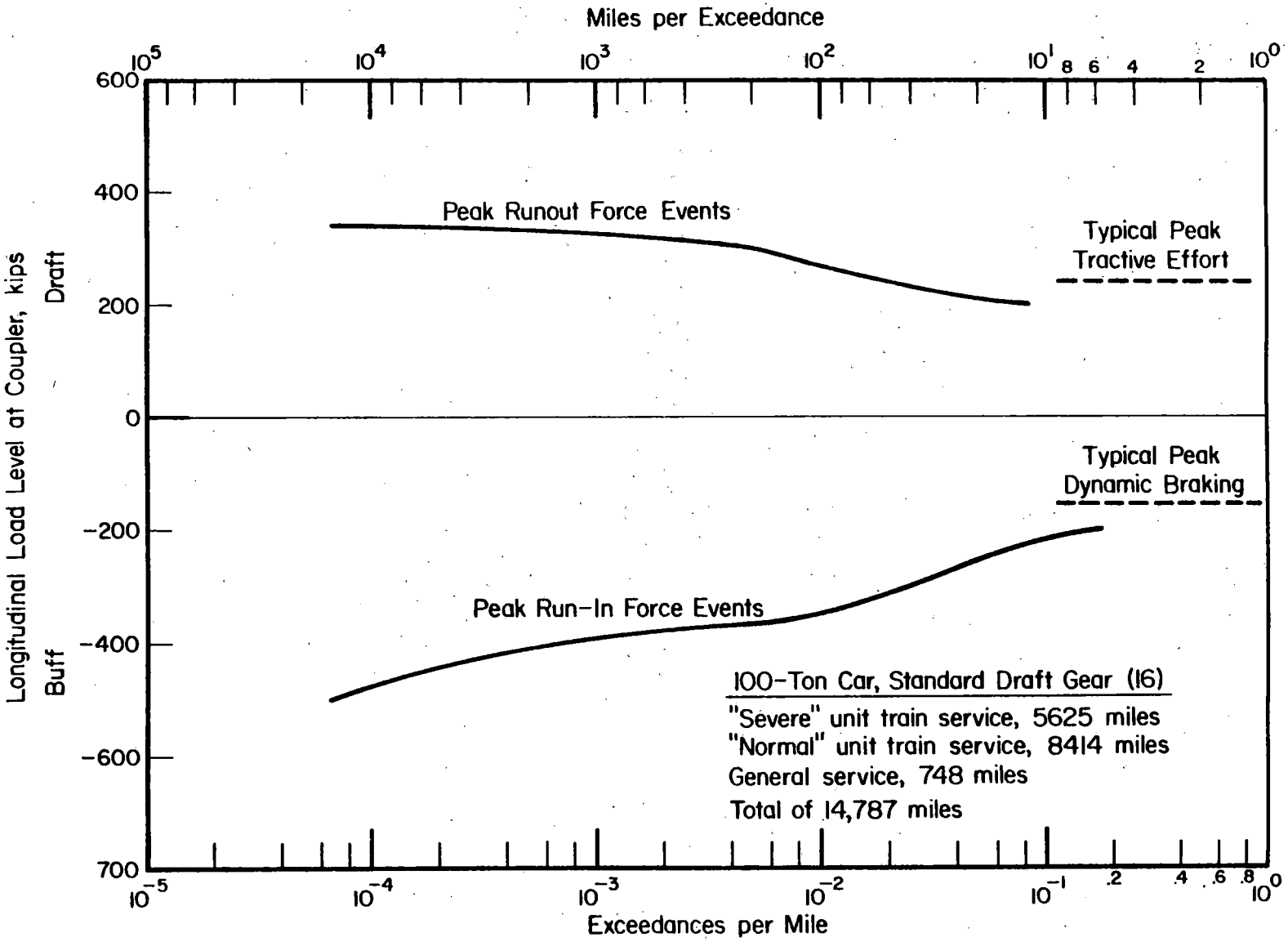

FIGURE 8. TYPICAL SERVICE LONGITUDINAL LOAD ENVIRONMENT ON DRAFT GEAR OF 100-TON CAR

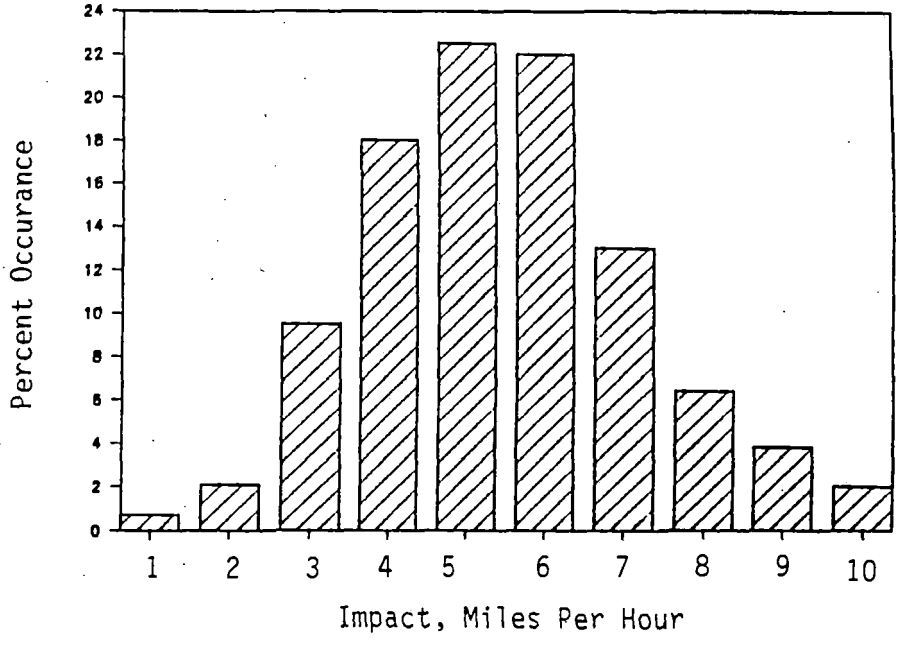

FIGURE 9. DISTRIBUTION OF MEASURED TANK CAR IMPACT VELOCITIES[17]

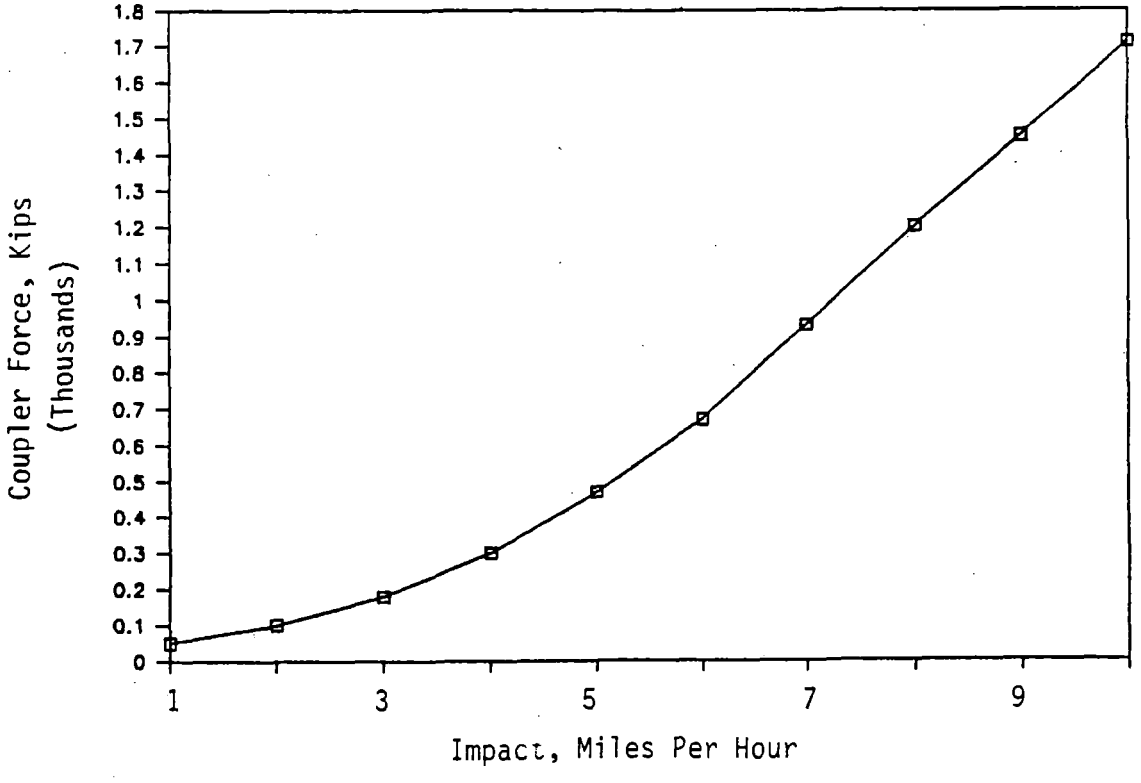

FIGURE 10. CORRELATION BETWEEN TANK CAR IMPACT VELOCITY AND COUPLER FORCE

The use of coupler vertical restraint systems on hazardous-material tank cars results in significantly higher vertical loads on the coupler that will induce pitch-plane bending moments on the draft gear. This will tend to move the vertical load on the centerplate to the front or rear edge. Limited data were available from AAR Report No. R-245[18] describing this loading in a statistical sense.

The AAR has reported that vertical loads on an F type coupler can reach as high as 50,000 lbs. For the purpose of fatigue life prediction, the plot in Figure 11 was extrapolated to this load level. Because this extrapolation is not based upon any frequency information and can lead to very damaging fatigue cycles, fatigue analyses were performed both with and without the extrapolated data.

Stress Analysis

A finite element stress analysis was completed on the 105A300W and 105A400W type cars manufactured by Richmond Tank Car Company. This class of car is the same type of car as the ECUX 575000 series cars owned and operated by Exxon Chemical Americas Company, Shell Oil, and Richmond Tank Car. (A schematic of the stub sill design was provided in Figure 1.) It is virtually identical to the BCDX 498 105A300W car owned and operated by Borden Chemical Co., with the exception of a thinner shell wall, as allowed by the 300 psi test pressure. (As mentioned earlier, BCDX 498 suffered a leak in Seattle, Washington in 1985.)

The finite element model was designed to take advantage of symmetry by considering one-quarter of the shell and one-half of the truck and stub sill. The shell and attached structures were represented by 3-D thick shell elements with active grid points at the corner nodes and three numerical integration points per element side.

The stub sill and bolster pads were represented as an overlaid set of shell elements, sharing common nodes with the tank shell at the weld lines. At interior locations, the pads are defined by nodes coincident with the shell nodes.

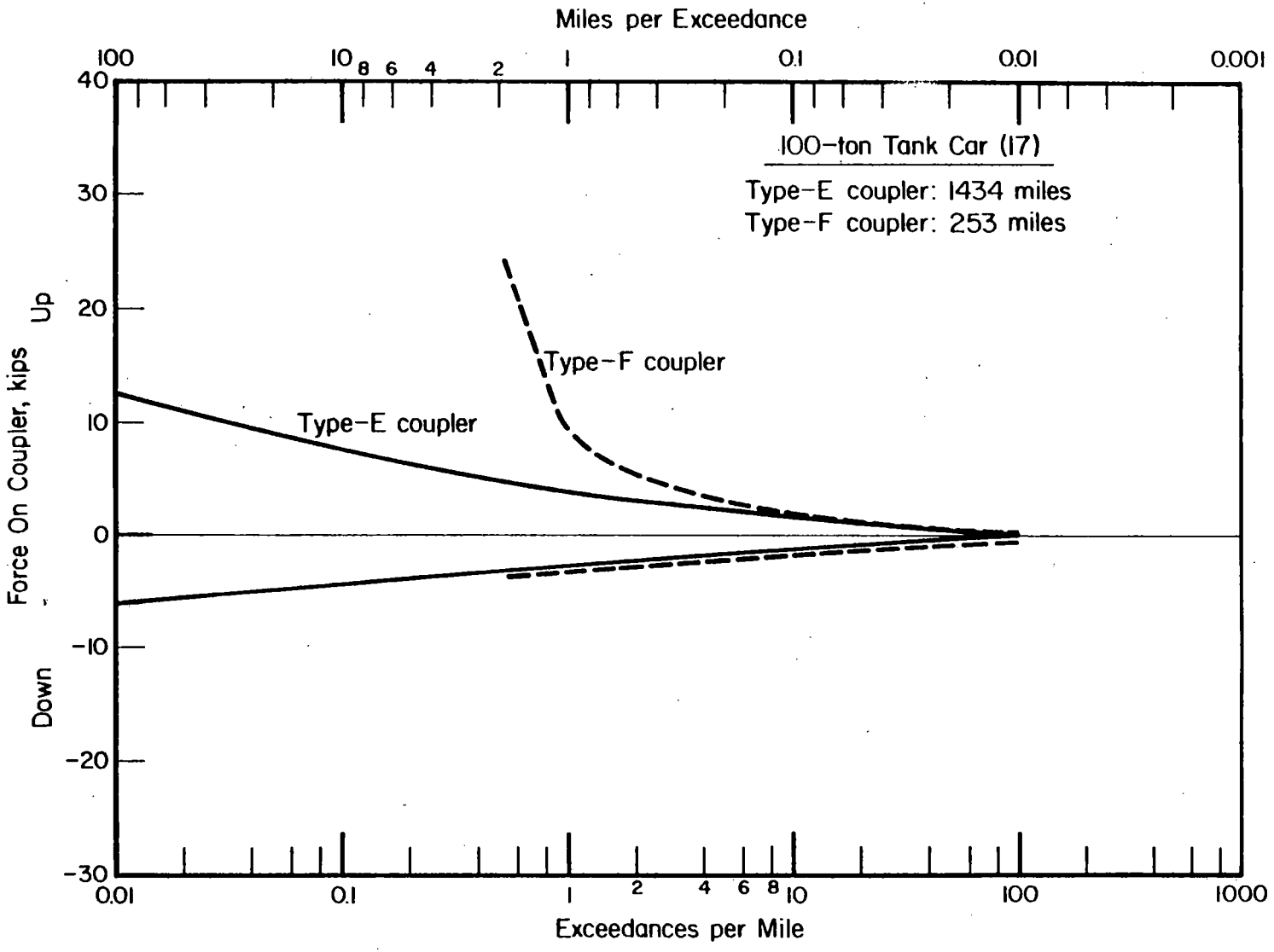

FIGURE 11. VERTICAL FORCES IN TYPE E AND F COUPLERS

The bolster and stub sill were treated as plate-like structures, with some minor structural details omitted for expediency.

The current repair procedure for the Richmond cars consists of a front bolster pad extension and a gusseted head brace. These members were included in the first level model. The initial analysis was performed on the as-designed configuration. The material properties associated with the elements representing the additional repair structure were very "soft" in this analysis to make their structural contribution negligible. The actual material properties were then incorporated for subsequent analyses to determine the effect of the repairs.

The tank and reinforcement pad interface was modeled as overlaid elements using coincident nodes in the pad region. The weld lines were again modeled using common nodes as with the bolsters. In conversations with the FRA inspectors, it was stated that only cars with poor-fitting pads were found to have cracks. For cars with a good fit between the tank and pad, no cracks were discovered. A typical fit was defined as a gap between the tank and pad of 3/8 to 1/2 inch, whereas a good fit would be approximately 1/32 inch.

To properly account for the gap between the tank and pad in the finite element model, two options were available. The first, as originally proposed, was to create a number of different pads with varying gap sizes. A tension-only restraint between the nodes in the pad and the nodes in the tank could also be employed. This restraint would have allowed the tank and pad elements to separate when in tension, such as during draft loads, and would restrict overlapping when in compression, such as buff forces or coupling. Unfortunately, the use of the tension-only restraint proved to be cost prohibitive because of the nonlinearity of the analysis and the extensive modeling effort required to create the different pads.

The second option, that was used in this study, was to use coincident nodes without the tension-only constraint. The implication of using coincident nodes without the tension-only constraint is that overlapping between the tank and pad elements is permitted. This overlapping in compression effectively simulates the presence of a gap

between the tank and the reinforcing pad. The overlap displacements were checked with each longitudinal load analysis to ensure that they did not exceed a worst case gap of 1/2 inch during a one-million-pound loading. However, the actual overlap was generally on the order of 1/50 inch. The potential impact of poor fitting reinforcement pads is discussed further in a later section titled Sources of Uncertainty.

Fatigue Life Estimation

Background

The model used to predict the fatigue lives of the tank car weldments consists of two parts; the predicted crack initiation life, N_i, in cycles, and the predicted crack propagation life, N_p, in cycles. The sum of these two components is considered to be the total life, N_t.

$$N_t = N_i + N_p \ . \qquad (1)$$

The crack initiation life is estimated using local strain fatigue concepts and the crack propagation life is estimated using fracture mechanics concepts. These concepts are presented in this section as they generally apply to fatigue life estimation for notched components or specimens.

Initiation Life Model

Fatigue cracks generally initiate at a geometrical discontinuity such as a notch or weld toe. These act as stress concentrations, raising the stress in the region of the notch to levels above the nominal stresses. The material at the weld toe may deform plastically while the rest of the component remains essentially elastic. Subjecting the region to cyclic loading may cause plastic deformation that will eventually result in a fatigue crack.

Determining the stress-strain state in a notch region (such as a weld toe) after the onset of local plasticity requires a notch analysis technique. In the elastic range, the notch stress can be calculated using the elastic stress concentration factor, K_t. The K_t value is simply a conversion factor between notch stresses and remote stresses,

$$\Delta\sigma = K_t \Delta S \tag{2}$$

and can be determined by elasticity theory or by finite element analysis. After material in the notch region deforms plastically, however, the elastic stress concentration factor no longer applies as a direct conversion factor. The stress will rise at a lesser rate and the strain at a greater rate than during elastic deformation, where both stress and strain rates were equal. To solve this problem, Nueber's[19] rule can be used. Nueber's rule states that the elastic stress concentration, K_t, will remain equal to the geometric mean of the instantaneous stress and strain concentration factors, K_σ and K_ϵ, respectively,

$$K_t = (K_\sigma \, K_\epsilon)^{1/2} \quad . \tag{3}$$

Rewriting this relation as

$$K_t = \left(\frac{\Delta\sigma \, \Delta\epsilon}{\Delta S \, \Delta e} \right)^{1/2}$$

where ΔS is the nominal stress range, and Δe is the nominal strain range, and recalling that

$$\Delta e = \Delta S / E \tag{4}$$

where E is the elastic modulus, Neuber's rule may be written as

$$\frac{\Delta S^2 \quad K_t^2}{E} = \Delta\sigma \, \Delta\epsilon \quad .$$

This expression relates the local stress-strain response at the notch root to the nominal stress and elastic stress concentration factor. Furthermore, representing the stress-strain response of the material with power law hardening constants,

$$\Delta\epsilon = \frac{\Delta\sigma}{E} + \left(\frac{\Delta\sigma}{K}\right)^{1/n} \tag{5}$$

where K is the strength hardening coefficient, and n is the strain hardening exponent, the relation can be written with $\Delta\sigma$ as the only unknown,

$$\frac{\Delta S^2}{E} \quad K_t^2 = \Delta\sigma \left[\frac{\Delta\sigma}{E} + \left(\frac{\Delta\sigma}{K}\right)^{1/n}\right] .$$

Solving for $\Delta\sigma$ can be accomplished using an iterative technique such as Newton's method.

In fatigue testing, it is generally observed that the actual lives of notched components are somewhat longer than would be expected for the notch root stress calculated using the elastic stress concentration factor, K_t. That is, notches have a less detrimental effect on fatigue life than would be predicted. This effect is dependent upon both defect size and material. To account for this difference, a fatigue notch factor, K_f, is often used in place of K_t for fatigue life predictions. The fatigue notch factor is defined as

$$K_f = \frac{\text{unnotched stress at a finite life (e.g. } 10^7\text{)}}{\text{notched stress at the same life}} . \tag{6}$$

The value of K_f for a given notch geometry and material can be determined experimentally or by the use of analytical relations. A commonly used fatigue notch factor relation is Peterson's[20] equation,

$$K_f = 1 + \left[\frac{K_t - 1}{1 + a/r}\right] , \tag{7}$$

where a is a material constant dependent on strength and ductility and r is the notch tip radius. The material constant "a" can be approximated for ferrous-based wrought metals by an equation fitted to Peterson's data,

$$a = \left[\frac{300}{S_u} \right]^{1.8} \times 10^{-3} \text{ in.} \qquad (8)$$

where S_u is the ultimate strength of the material in ksi units. Peterson's equation implies that small notches are least sensitive in fatigue, and that ductile materials are less sensitive to notches in fatigue than strong materials.

Using Nueber's rule for notch root stress-strain behavior, along with Peterson's equation for the fatigue notch factor, it is possible to predict the stress-strain response of the notch root material subjected to fatigue loading. It still remains to relate these local stresses and strains to actual fatigue life data. Because the plastically deformed notch root material is constrained by the surrounding elastic material, the notch root is nearly in a strain-control condition. Therefore, it is commonly assumed that the notch root material is essentially cycled between strain limits analogous to that experienced by a material in strain-control, low cycle fatigue testing. The assumption, therefore, is that strain-life fatigue data obtained using unnotched, low cycle fatigue specimens can be used to predict the cycles to crack initiation, N_i, at a notch root. Low cycle fatigue strain-life data are often represented by the Coffin-Manson[21] equation, with Morrow's[22] mean stress correction as follows:

$$\frac{\Delta\epsilon}{2} = \epsilon_f'(2N_f)^c + \left(\frac{\sigma_f' - \sigma_m}{E} \right)(2N_f)^b \qquad (9)$$

where $\Delta\epsilon/2$ is the strain amplitude, ϵ_f' is the fatigue ductility coefficient, σ_f' is the fatigue strength coefficient, σ_m is the mean stress,

$2N_f$ is the reversals to failure, c is the fatigue ductility exponent, and b is the fatigue strength exponent. By relating the strain calculated at the notch root to the strain-life data, the number of cycles to initiate a fatigue crack at the notch can be estimated. This is the basis of the initiation life predictions. The strain-life data parameters, ϵ_f', σ_f', c, and b, are obtained either by low cycle fatigue testing or by using estimates.

Hardness measurements are often used to estimate fatigue properties of weldments in lieu of mechanical testing to determine properties. Since fatigue cracks generally initiate in the relatively narrow metallurgical region of the heat affected zone, direct testing is difficult. A number of relationships between fatigue properties and hardness have been established and are presented below:

Ultimate strength, MPa:

$$S_u = 6.9\ HB/2$$

Cyclic yield strength, MPa:[23]

$$\sigma_y' = 0.608\ S_u$$

Fatigue strength exponent:[24]

$$b = -1/16 \log (2.1 + 917/S_u)$$

Fatigue ductility exponent:

c varies between -0.5 for hard steels and -0.7 for ductile steels

Cyclic strain hardening exponent:[25]

$$n' = b/c$$

Cyclic strength coefficient:

$$K' = \sigma_y\ (0.002)^{-n'}$$

Fatigue strength coefficient, MPa;[20]

$$\sigma_f' = 0.95\ Su + 370$$

Hardness data for weldments on typical tank car steels (ASTM 515 and TC 128-B) are presented in Table 1 along with the estimated fatigue properties. The AAR[26] and GE[27] data are for TC 128-B. The AAR data were obtained from weldments with no prior loading history and the GE

TABLE 1. ESTIMATED FATIGUE PROPERTIES OBTAINED FROM HARDNESS MEASUREMENTS

Data Source and Material	Weld and Heat-Affected-Zone Identification	Brinnel Hardness HB	Ultimate Strength S_u, ksi (MPa)	Cyclic Yield Strength σ'_y, ksi (MPa)	Fatigue Strength Cofficient σ'_f, ksi (MPa)	Fatigue Strength Exponent b	Fatigue Ductility Coefficient ϵ'_f	Fatigue Ductility Exponent c	Cyclic Strength Coefficient K, ksi (MPa)	Cyclic Strain Hardening Exponent n'
AAR	TA, Bead, 1100 F, 1 hour	255	127.5 (880)	77.5 (535)	175 (1206)	-0.083	0.719	-0.6	183 (1262)	0.138
(TC-128B)	TA, Bead, 1200 F, 1 hour	254	127 (876)	77.2 (533)	174 (1202)	-0.083	0.720	-0.6	182 (1258)	0.138
	TA, Butt, SMW, 1200 F, 1 hour	263	131.5 (907)	79.9 (551)	178 (1231)	-0.082	0.708	-0.6	187 (1291)	0.137
	TA, Butt, SAW, 1200 F, 1 hour	268	134 (925)	81 (562)	181 (1249)	-0.082	0.701	-0.6	190 (1311)	0.137
GE	Seam Weld	187	93.5 (645)	56.8 (392)	142 (983)	-0.091	0.847	-0.6	146 (1008)	0.152
(TC-128B)	Heat-To-Plate Weld	216	108 (745)	65.6 (453)	156 (1078)	-0.087	0.784	-0.6	162 (1116)	0.145
Canada	Sill Pad Extension to Original Sill	170	85 (586)	51.6 (356)	134 (926)	-0.094	0.892	-0.6	137 (943)	0.157
(A-515-70)	Original Sill Pad to Original Tank	170	85 (586)	51.6 (356)	134 (926)	-0.094	0.892	-0.6	137 (943)	0.157
	Sill Pad Extension to Tank Insert Material	142	71 (490)	43.2 (298)	121 (835)	-0.100	0.984	-0.6	121 (838)	0.167

data were obtained from a cracked weldment taken from a tank car. As would be expected, the GE weldment apparently incurred some cyclic softening (note the lower hardness values). The welds subjected to actual service conditions should provide more realistic results and thus they were used in fatigue life predictions.

The Canadian Transport Commission Report[28] contained data on weldments with A515-70 steel also subjected to service loadings. The A515-70 weldments exhibited a lower mean hardness than the TC 128-B weldments (161 vs. 201HB). The reinforcement pad on tank cars are usually fabricated from A515-70. The sill-to-pad weld, which is considered critical, is cracking on the pad side of the weld at the toe. Therefore, A515-70 hardness measurements were used to estimate the fatigue properties of this critical weld.

Propagation Life Model

Paris and Erdogan have shown that fatigue crack growth rates are dependent upon the stress intensity associated with the fatigue crack tip. The power-law relationship is of the form

$$\frac{da}{dN} = A\ \Delta K^{m} \quad , \tag{10}$$

where da/dN is the fatigue crack growth rate, ΔK is the stress intensity factor range, and A and m are material constants dependent upon environment, stress ratio, temperature, and frequency. The growth rate expression used throughout this study has a correction factor to account for mean stress effects,

$$\frac{da}{dN} = \frac{A\ \Delta K^{m}}{1-R} \quad ,$$

where R is the stress ratio. The crack growth constants "A" and "m" used in this tank car study were the same as used in a DOT tank car shell cracking and structural integrity assessment[29], which were

obtained from Rolfe and Barsom[30] as lower bound values for pearlitic steels. These are

$$A = 3.6 \times 10^{-10}$$
$$m = 3$$

The general relationship for the stress intensity factor range is written as

$$\Delta K = Y \Delta S (\pi a)^{1/2} , \qquad (11)$$

where Y is a geometry dependent factor, ΔS is the stress range, and "a" is the crack length. The solution for the stress intensity of a semi-elliptical crack in a plate was used in this study to model a fatigue crack growing through the reinforcing pad. Such a solution is found in Rooke and Cartwright[31] for both axial and bending loads.

The estimated crack propagation life is strongly dependent upon the initial crack size that is chosen. The initial crack sizes used for this study were taken as the expected size of the plastic zone of the weld toe under the given loading history. This approach weights the initial crack size more strongly to the load cycles most responsible for the crack initiation fatigue damage.

Loading Spectra

The loading spectra for the longitudinal coupler, the vertical coupler and the vertical centerplate loads were converted into stress cycles as determined by the finite element analysis. Each of the three spectra were assumed to act independently of one another, with the possibility of simultaneous loadings considered very remote. There is, however, the possibility of a mean longitudinal stress superimposed upon the vertical (over-the-road travel) loading events. This stress is essentially the draft load realized in the draft gear as the train is moving. A mean stress is generally detrimental from a fatigue stand-

point. As seen in Figure 12[10] the draft load decreases markedly with increased speed. Although this tractive effort curve applies only to cars at the head end of the consist, it presents the worst case loading, which was considered appropriate for this failure scenario. Fatigue analysis cases were run both with and without a longitudinal mean stress to assess the significance of this variable. The mean stress casess assumed a single locomotive travelling at a speed of 45 mph resulting in a tractive load on the first drawbar in the consist. This resulted in approximately a 10 ksi mean stress at the critical sill-to-reinforcing pad interface location. (The speed of 45 mph represents an average for freight rail travel.)

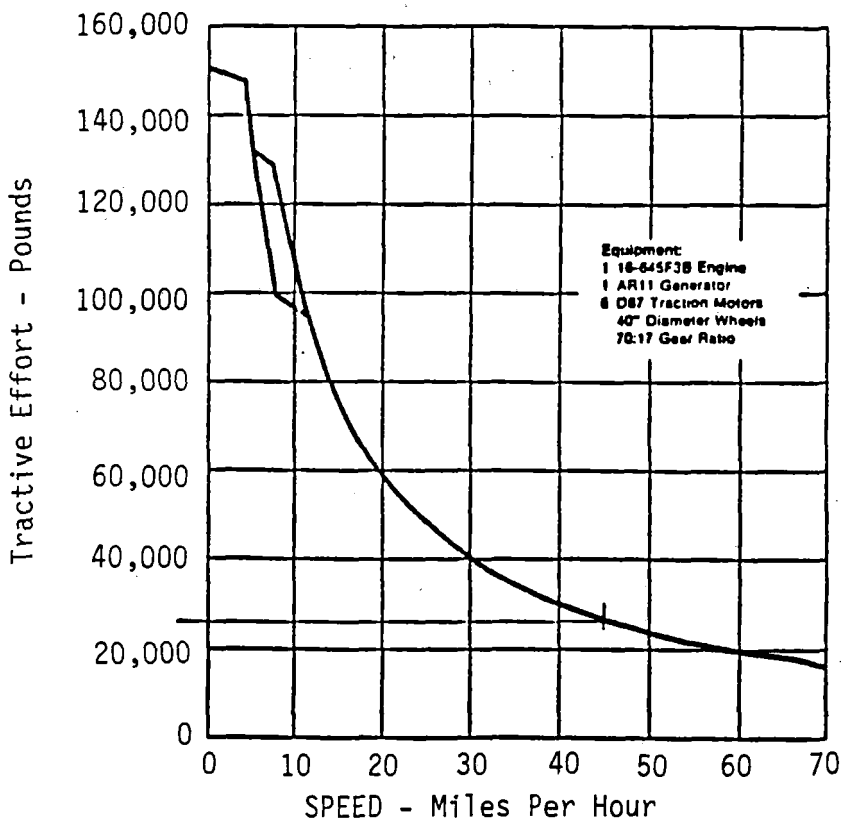

FIGURE 12. TRACTIVE EFFORT VS. SPEED FOR A LOCOMOTIVE SHOWING THE PRESENCE OF A MEAN STRESS DUE TO LONGITUDINAL COUPLER LOADS

ANALYSIS RESULTS

Richmond 300W and 400W Designs

Stress Analysis and Results

The Richmond 300W and 400W finite element models are shown in Figure 13. Figure 13, shows the overall mesh including the tank, sill and bolster substructures. Figures 14 and 15 show the sill and bolster assembly details respectively.

The remote stresses in the reinforcing pad near the pad-sill interface where crack initiation has occurred were analyzed for the three types of loading being considered; longitudinal sill loading, vertical center plate loading, and vertical coupler loading. For each loading type, a loaded tank car was assumed. The nominal static load at the center plate was assumed to be 120,000 pounds per truck for both the loaded 300W and the loaded 400W car. The loaded condition was achieved by assuming a 32 ft/sec/sec (1 g.) downward acceleration on all elements. The density of the elements in the lower half of the tank were increased to simulate a tank with a liquid load. In the unloaded condition, the static load at the center plate for the 400W and 300W cars were assumed to be 59,000 pounds and 22,750 pounds, respectively. To determine stresses in the vicinity of the sill pad weld, a two dimensional finite element model using quadrilateral plane strain elements was used. The displacements calculated from the three dimensional tank model were applied to the two dimensional weld detail as input boundary conditions. Displacements were used as inputs so that the two dimensional model would produce the equivalent deformation as the three dimensional model. This was done because the two dimensional elements could be more highly refined than the shell elements and the nominal stresses in the pad and the stress concentration and gradient could be more accurately determined.

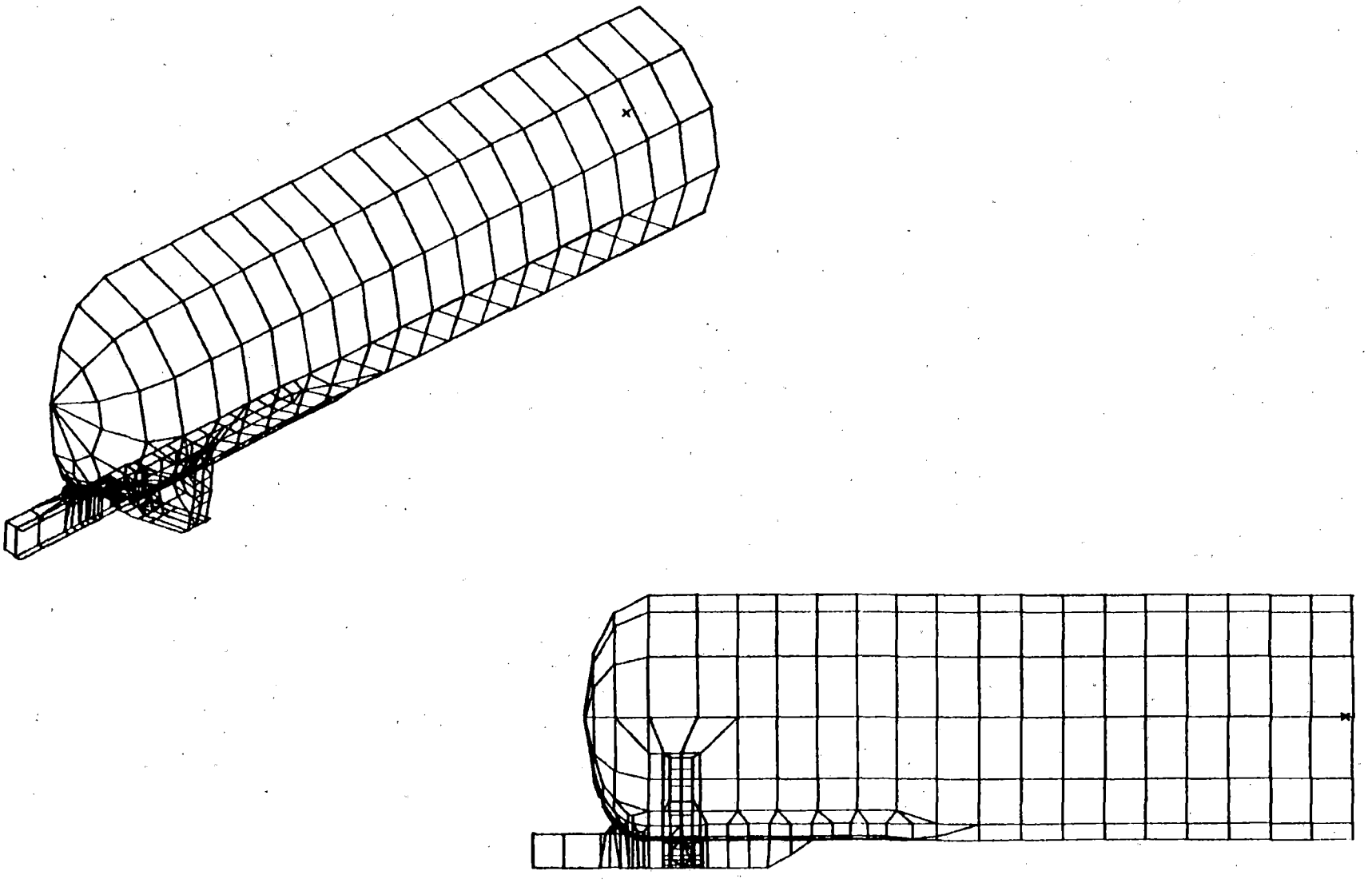

FIGURE 13. FINITE ELEMENT MESH FOR RICHMOND 300W TANK CAR

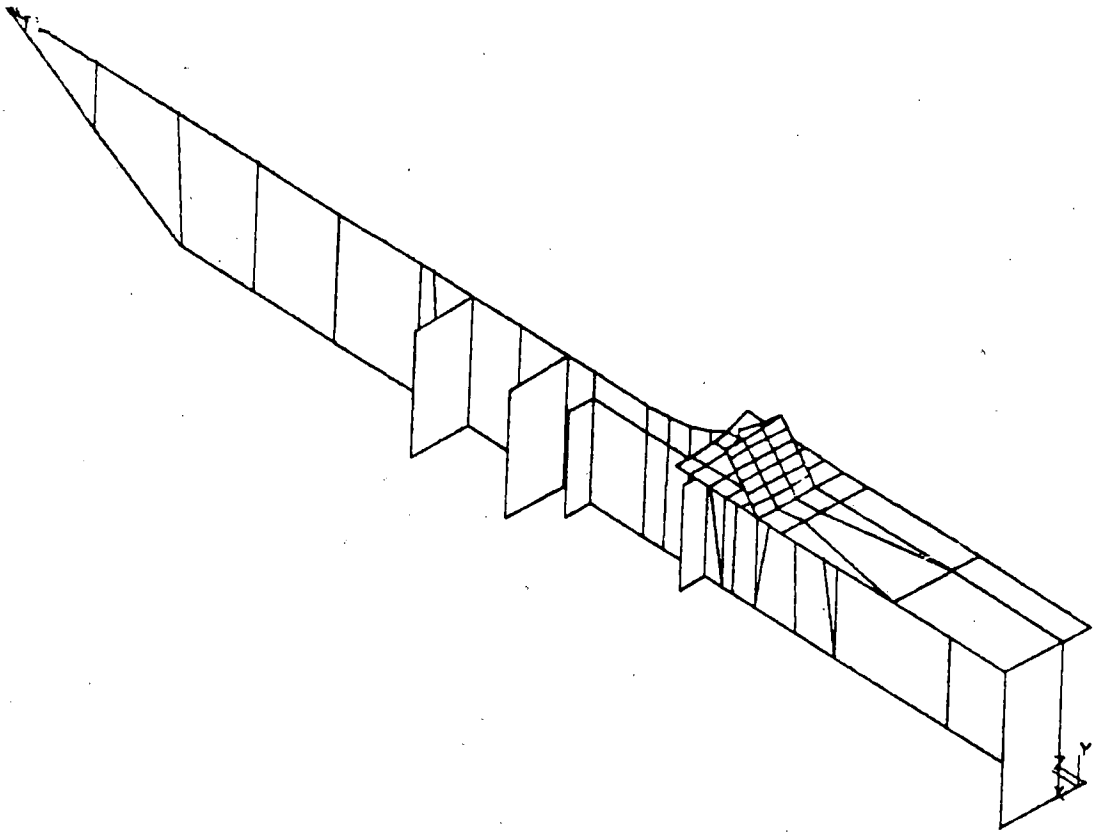

FIGURE 14. RICHMOND 400W SILL SUB-STRUCTURE

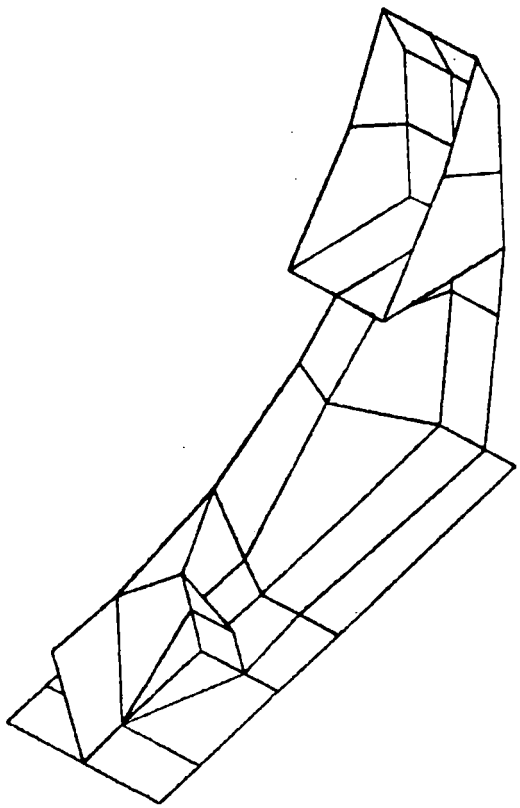

FIGURE 15. RICHMOND 400W BOLSTER SUB-STRUCTURE

The nominal stresses in the reinforcing pad were found from an examination of the principal stress gradient through the thickness of the plate. It has been shown that the stress levels due to the stress concentration at the weld decrease to nominal stress levels at a depth of about 0.3 of the plate thickness[32]. Figure 16 shows the principal stress gradient throughout the thickness of the reinforcing pad for the 400W as built car with a 1000 kip longitudinal coupler load. The plot shows that the face of the pad on the opposite side of the weld is in compression and the weld side is in tension. The nominal stress shown, therefore, consists of both an axial component S_A, and bending component S_B where

$$S_{nom} = S_A + S_B \quad . \tag{12}$$

The axial and bending components can be decomposed as follows.

The minimum principal stress at the face away from the weld ($t/t_o = 1$, where t_o is the plate thickness and t is the distance from the weld toe) is the maximum compressive stress of the outer fiber. The maximum principal stress at $t/t_o = 0.3$ is the maximum tensile stress which is not affected by the stress concentrating effects of the weld toe. The line drawn through these points is the summation of the axial and bending components of principal stress through the plate. Assuming that the neutral axis due to bending coincides with the midplane, there should be no bending component contributing to the stress at this point. Therefore the stress at this point is due solely to the axial component, S_A. The bending component is therefore

$$S_B = S_{nom} - S_A \qquad \text{at } (t/t_o = 0) \quad . \tag{13}$$

This procedure was used in determining the nominal stress values in all loading cases. The results are summarized in Tables 2 and 3. Note the decrease in nominal stress for the repaired condition.

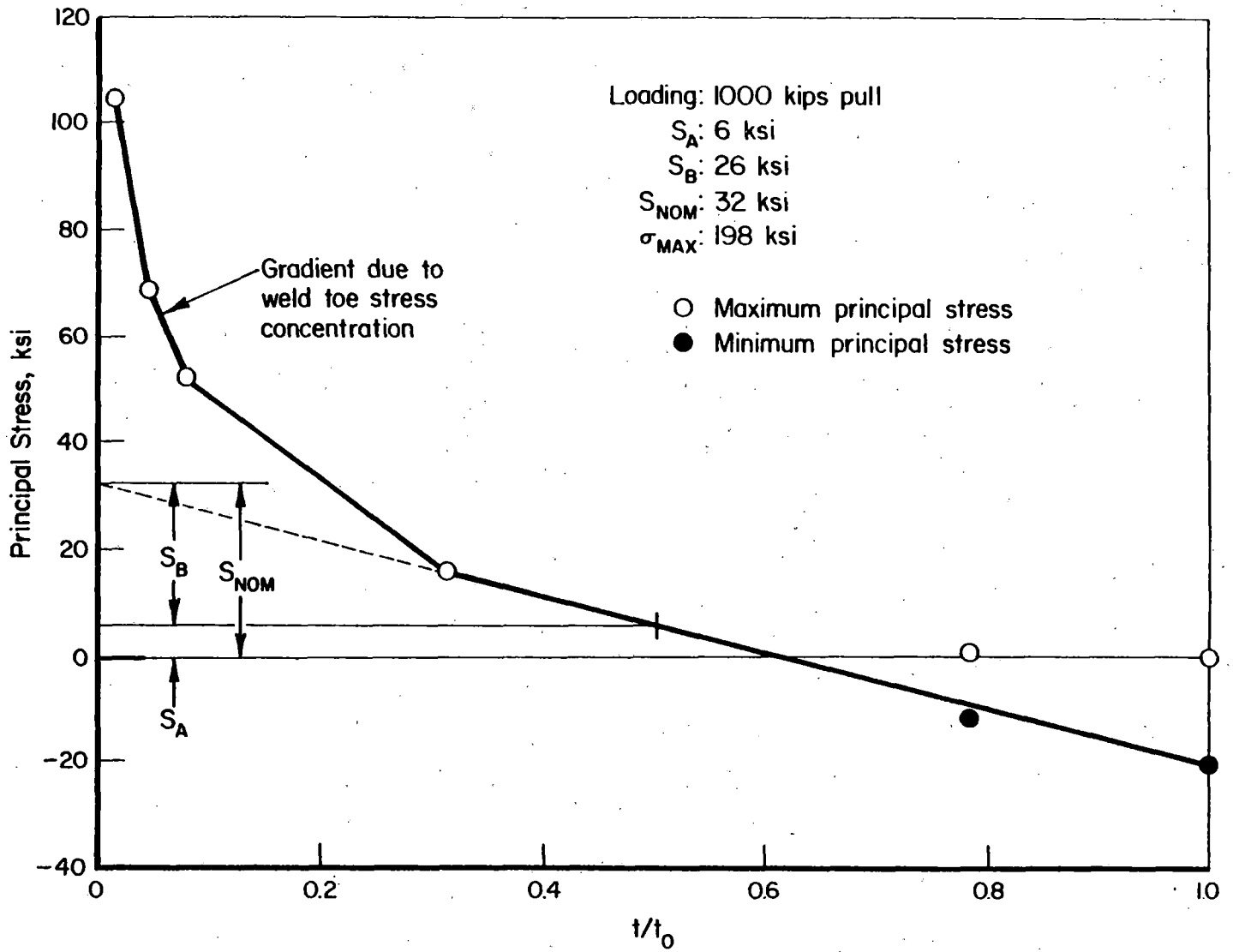

FIGURE 16. PRINCIPAL STRESS GRADIENT THROUGHOUT THE THICKNESS OF THE REINFORCING PAD FOR THE 400W CAR AND A 1000 KIP LONGITUDINAL PULL LOAD, AS BUILT. t_o IS THE PAD THICKNESS. t IS THE DISTANCE FROM THE WELD TOE

TABLE 2. RICHMOND 300W TANK CAR STRESS ANALYSIS

	S_{Axial} as Built (ksi)	S_{Axial} Repaired (ksi)	Percent Change	$S_{Bending}$ as Built (ksi)	$S_{Bending}$ Repaired (ksi)	Percent Change	S_{nom} as Built (ksi)	S_{nom} Repaired (ksi)	Percent Change
Loading									
Longitudinal 1000 kip pull	8	11	+37	32	20	-37	40	31	-22
Vertical Center Plate 1 kip	-2	-1	-50	-2	-1	-50	-4	-2	-50
Vertical Coupler 50 kip up	0	2	+100	-40	-11	-72	-40	-9	-77.5

TABLE 3. RICHMOND 400W TANK CAR STRESS ANALYSIS

	S_{Axial} as Built (ksi)	S_{Axial} Repaired (ksi)	Percent Change	$S_{Bending}$ as Built (ksi)	$S_{Bending}$ Repaired (ksi)	Percent Change	S_{nom} as Built (ksi)	S_{nom} Repaired (ksi)	Percent Change
Loading									
Longitudinal 1000 kip pull	6	9	+50	26	19	-27	32	28	-12
Vertical Center Plate 1 kip	-2	-1	-50	-3	-1	-67	-5	-2	-60
Vertical Coupler 50 kip up	0	2	+100	-40	-10	-75	-40	-8	-80

The two dimensional weld details were generated with a weld toe radius of 0.008 inches. This radius was chosen in accordance with the maximum fatigue notch factor, $K_{f_{max}}$, concept used to predict fatigue crack initiation in weldments[26]. The elastic stress concentration, K_t, at the weld toe increases with decreasing weld toe radius. In fatigue, however, it is generally observed that a decreasing notch root radius reaches a limiting condition as to its effect on fatigue life. Lawrence[26] has shown that for a given material there exists a worst case notch root size (the weld toe in the case of welds), which will control fatigue life. The critical weld toe size is equivalent to the material parameter, a, in Peterson's equation for the fatigue notch factor

$$K_f = 1 + \left[\frac{K_t - 1}{1 + a/r}\right] \quad , \tag{7}$$

where r is the weld toe radius. By differentiating this relationship with respect to r, it can be shown that the maximum value of the fatigue notch factor, $K_{f_{max}}$ occurs at r = a. The material parameter, "a" can be approximated for ferrous-based wrought metals by an equation fitted to Peterson's data,

$$a = \left[\frac{300}{S_u}\right]^{1.8} \times 10^{-3} \text{ in} \quad , \tag{8}$$

where S_u is the ultimate strength (in ksi) of the heat affected zone at the weld toe, (see Table 1). Using the ultimate strength value of 108 ksi, the resulting value of "a" equals approximately 0.008 inches; the value used as the weld toe radius. Using this radius to determine the stress concentration, one can easily calculate the maximum fatigue notch factor as

$$K_{f_{max}} = 1 + (K_t - 1)/2 \quad .$$

Fatigue Life Estimates

The fatigue life estimates for the Richmond 300W and 400W tank cars were calculated for both good welds and undercut welds, with and without the mean stress from 45 mph train speeds. Estimates were calculated with loads data compiled from documented service, noted as the regular history and the history with the Richmond Impact Data and the verbal report of vertical coupler loads from the AAR as the severe history.

The material properties data used in these analyses were estimated for the hardness data from the A515 welds reported in the Canadian Railway Report[21]. These were the only hardness data available for A515 material. These data are identified in Table 1 as the original sill pad to original tank data.

The residual stress in the sill-to-reinforcing pad weld was assumed to be zero due to post weld heat treatment. Section AAR.100-11 of the AAR Manual of Standards and Recommended Practices; Specification for Tank Cars[32] states "the portions of carbon steel tanks to which anchorge or draft sills are attached must be postweld heat treated" for relief of residual stresses due to welding. Although heat treating will not remove all the residual stresses due to welding, the residual stress state will be markedly reduced. Therefore, residual stresses were not included in the fatigue life calculation, i.e. in Equation 9, the residual or near stress term, σ_a, was set equal to zero.

The undercut weld fatigue life estimates were calculated using a procedure developed by Lawrence[33]. The technique uses elastic superpositon to determine the stress concentration value, K_t, of a notch in a weld toe. The stress concentration of the undercut, K_{tu}, is multiplied by the maximum principle stress value of the weld toe stress gradient, S_g, without the undercut,

$$K_t = K_{tu} \times S_g$$

where

$$K_{tu} = 1 + 2\sqrt{d/r} \quad .$$

In the preceding equation, d is the depth of the undercut and r is the radius of the undercut tip. All undercut calculations were made assuming an 0.1 inch deep undercut with a tip radius of r = 0.01 inch. The resulting K_{tu} is 7.32. The value of S_g is dependent upon the loading mode.

The fatigue life estimate results are given in Tables 4 and 5. The values reported here are the fatigue crack initiation estimates only. These estimates can be compared with actual estimates of service at the time cracks were found in the field -- 30,000 to 250,000 miles.

TABLE 4. FATIGUE LIFE ESTIMATES FOR 300W DESIGN

Richmond 300W	Service Miles	
As Built		
Zero Mean Stress	Severe History	Regular History
Good Weld	280,000	1,895,000
Undercut Weld	10,000	25,000
10 ksi Mean Stress	Severe History	Regular History
Good Weld	180,000	1,190,000
Undercut Weld	10,000	25,000
REPAIRED		
Zero Mean Stress	Severe History	Regular History
Good Weld	31,950,000	41,505,000
Undercut Weld	145,000	145,000
10 ksi Mean Stress	Severe History	Regular History
Good Weld	31,950,000	41,505,000
Undercut Weld	145,000	145,000

TABLE 5. FATIGUE LIFE ESTIMATES FOR 400W DESIGN

Richmond 400W		
As Built	Estimated Miles to Crack Initiation	
Zero Mean Stress	Severe History	Regular History
Good Weld	320,000	4,720,000
Undercut Weld	15,000	60,000
10 ksi Mean Stress	Severe History	Regular History
Good Weld	190,000	1,865,000
Undercut Weld	15,000	60,000
REPAIRED		
Zero Mean Stress	Severe History	Regular History
Good Weld	>5,000,000	>5,000,000
Undercut Weld	285,000	295,000
10 ksi Mean Stress	Severe History	Regular History
Good Weld	>5,000,000	>5,000,000
Undercut Weld	285,000	295,000

All crack propation estimates resulted in cracks requiring over five million miles of service at the load levels from the defined load spectra. This means, that, even though fatigue cracks were predicted to initiate under the loading spectra compiled, the cracks would not be expected to grow to a critical failure size in any reasonable length of time. This result is clearly inconsistent with the service history cracking reported in the Richmond cars in Table 6. These service data were reported in Richmond's evaluation of the tank car designs. It must therefore be concluded that some aspect of the

service conditions are not being accounted for in the present analysis. Some of these possibilities are explored below.

Dynamic Loading. The inability of the static analysis to account for vibration induced stresses could lead to unconservative crack growth estimates. As discussed earlier in this report, a poor fitting reinforcement pad could result in a significant vibratory stress upon impact loading. In the Richmond study[17], the laboratory testing included strain gaging the reinforcement pad and measuring strains during impact loading. The impacts resulted in a vibration in the pad (without the head brace). This vibratory load is not included in the present study's loading spectra. In fact, the impact loads are not contributing to the crack initiation damage very significantly because the events are relatively few in number and the impact coupling load results in a compressive stress at the weld toe. A reflected stress wave from a dynamic impact would result in a crack opening tensile stress, contributing much more damage both for crack initiation and propagation.

Material Properties. The crack growth constants "A" and "m" used in the analysis are reported as lower bound or "worst case" values. Unless the A515 material is abnormally poor in resistance to fatigue crack growth, the crack growth estimates would not underestimate the reality by such a large margin.

GATX Tank Car

Two tank car cracking incidents involving GATX cars have occured in recent years (FRA Memorandum 3666-RMJ-330 and 3666-RVK-91). Both incidents involved cracking of the transverse weld joining the reinforcement pad at the tank. This mode of cracking is critical

TABLE 6. ESTIMATED MILEAGE FOR CRACKED HEAD PAD CARS

Car No.	Est. Milage	Built Date	Car No.	Est. Milage	Built Date
RTMX 5217	33,200	1/81	RTMX 4218	93,700	3/74
RTMX 5218	36,000	1/81	RTMX 4508	94,600	1/76
RTMX 3B21	38,900	8/76	SOEX 3375	95,600	11/77
RTMX 4735	50,700	11/78	RTMX 3648	100,400	5/77
RTMX 4640	53,000	1/81	RTMX 4205	103,700	1/74
RTMX 4622 *	54,200	5/78	RTMX 4229	107,400	1/74
RTMX 5072	57,300	10/80	SOEX 3381	111,700	11/77
RTMX 4900	58,700	2/80	RTMX 3928	112,700	8/77
RTMX 4944 *	64,800	1/80	RTMX 4501	113,300	1/76
RTMX 4526 *	66,000	1/78	RTMX 3866	113,500	10/76
RTMX 3979	73,300	8/77	RTMX 4500	115,000	1/76
RTMX 4224	73,500	1/74	RTMX 3440	115,400	1/77
RTMX 4602 *	75,300	2/78	RTMX 4521	123,400	1/78
RTMX 4589	76,600	12/79	RTMX 3695 *	136,100	6/77
RTMX 3597	79,100	6/77	RTMX 3872	144,000	8/77
RTMX 3510 *	81,200	1/77	ECUX 575024	160,300	11/77
RTMX 4232	82,900	3/74	ECUX 575020	160,800	11/77
RTMX 3496	83,800	1/77	ECUX 575019	173,900	11/77
RTMX 3826 *	86,300	8/76	RTMX 3823	190,200	8/76
RTMX 4685 *	89,700	12/78	RTMX 3835	194,400	8/76
SOEX 3774	92,800	4/78	RTMX 3820 *	229,000	7/76
			RTMX 3804	252,000	

TOTAL = 43 Cars

Median = 93,700 Miles
Mean = 103,451 Miles
Lower 95% Confidence Limit = 88,797 Miles

NOTES: (1) Most cars had only 4-5 years of mileage data available. The average miles/year for this period was used to project total mileage for the life of the car.

(2) * - Cars that had surface or partial penetration cracks in the head or shell after cracked head pad was removed.

because crack growth through the tank wall results in leakage. The size of the reinforcement pad is considerably smaller in area than other manufacturer's designs. The GATX analysis involved a sensitivity study to investigate if an increased pad size would significantly reduce the stresses experienced in the critical weld. The original pad size was 14 inches wide by 18.5 inches long, with the front of the pad extending 1.75 inches beyond the head brace. The Richmond tank car finite element

model was modified to include a GATX vertical front face head brace, reinforcement pad, and cradle pad. A second model was also made with a larger reinforcement pad extending 6 inches forward of the transverse head brace weld, rather than the present design of 2 inches forward of the weld. The increased pad size is 14 inches wide by 23.5 inches long with the pad extending 6 inches beyond the head brace. The increased size pad has 26 percent more area and 16 percent more lineal weld (an additional 10 inches).

This finite element model was subjected to both a longitudinal coupler load (1,000,000 lbs) and a vertical coupler load (50,000 lbs.). The results are summarized in Table 7. The stress from the longitudinal load was decreased by 61 percent and the stress from the vertical loading was reduced by 34 percent. The reduction in stress near the weld would be expected to lessen the frequency of cracking at this location.

TABLE 7. GATX STRESS ANALYSIS SUMMARY

1,000 kip Longitudinal	Small Pad Max/Min Stress(ksi)	Large Pad Max/Min Stress(ksi)	Percent Change
Pull Load	26.0	14.1	-46
50 kip Vertical Coupler (up) load	-33.8	-22.2	-34

SOURCES OF UNCERTAINTY

A number of sources of uncertainty are inherent in the local strain fatigue analysis approach. A brief explanation of these follows, as well as estimates of the approximate magnitude of uncertainty of the results and the justification for using the approach rather than an alternate method.

(1) Static Finite Element Analysis

Although great pains were taken to model the stub sill tank car as closely as possible based upon Richmond Tank Car drawings, some geometrical error is inevitable. A problem that must be considered that was alluded to earlier, is the problem of poor fitting reinforcement pads. The finite element model was constructed with the pad and tank fitting perfectly, a condition seldom achieved in actual practice because of the difficult geometry.

All of the loads, except the gravity loading, were input as static loads. In reality, most of the significant loads that tank cars experience are dynamic, and these loads can result in stress waves propagating through the structure. Occasional large, impact loads may produce significant vibrations and local stresses that have not been accounted for in fatigue analyses at the critical locations.

The main reason that a static analysis was used rather than a dynamic analysis was the difficulty in accurately representing boundary conditions for the dynamic loading. When a tank car experiences a dynamic load, such as a coupling impact load, the resulting stress wave is not fully reflected upon impacting the next car in the consist. Rather, the stress wave is attenuated, and only partially reflected. The boundary conditions that must be used to model this condition are difficult to determine.

The static analysis should provide an accurate determination of the primary stresses. However, it should again be emphasized that vibration induced stresses are possible in the reinforcement pad as a result of impact loads.

(2) Local Strain Approach to Fatigue Analysis

The fatigue life estimation procedure that was used is based upon the local strain fatigue approach because this method accounts for the actual weld geometry and loading. In the Richmond Tank car analysis, the sill-to-reinforcement pad weld was modeled by a two dimensional finite element mesh to determine both the stress concentration factor and the resulting stress gradients. The weld toe radius was chosen from the K_f max concept as discussed in the fatigue analysis section. Because the material properties for the damage region must be estimated for the HAZ, there is some uncertainty in these estimates. However, for carbon steels, these properties have been shown to be a strong function of ultimate tensile strength and consequently, hardness measurements.

The alternative fatigue analysis procedure, preferred by the AAR, is the use of Goodman Diagrams for steel weldment details. This analysis procedure assumes that similar weld details will yield similar results for all carbon steels. The Goodman diagrams are based upon laboratory tests for the weld details to be analyzed. The obvious uncertainty involved with this analysis technique is that many weld details in tank cars and other structures are not amenenable to a standard laboratory weld detail. In this analysis, the critical location involves a fillet weld joining the sill and the reinforcing pad which is inclined at approximately 37° to the sill. This joint is not represented by any of the standard details for which Goodman Diagrams are available in the AAR Freight Car Manual.

(3) Compiled Loading History

The ideal method for collecting data for a stress spectrum for a fatigue analysis is to strain gage the region near the critical joint. When the car passes over

actual service track, the strains which are induced near the weld can be measured and reduced by a cycle counting procedure, such as rainflow counting, and used in a fatigue damage analysis. Unfortunately, the instrumentation and data collection procedure were beyond the scope of this and most other studies of this type. In recognition of this dilemina the rail community has funded programs such as FEEST to collect loads data for freight and tank cars subjected to actual service conditions. The alternative approach (used for this study) is a compilation of loads data and the use of finite element stress analysis to estimate the active stresses at the fatigue critical location.

Drawbacks to this approach are (1) the inability to account for stress interaction and phasing between loading modes, and (2) the difficulty in determining the stresses given only the loading. Addressing the first of these issues, the three loading modes analyzed in this study, (the longitudinal coupler, vertical coupler, and vertical centerplate loads) are generally thought to be independent. Because of the typically short duration of these loads, the possibility of simultaneous occurrence of the different loading modes is unlikely.

Mean stresses are of particular concern in regard to the second issue. The existence of mean stresses are to be expected. However, the only way to infer a mean stress is to physically rationalize such a mean stress through typical train operation. The presence of a mean stress upon stress cycles from the vertical loading modes due to the longitudinal mode is very likely. As shown in Figure 10, whenever the train cars are travelling, there is a mean stress in the longitudinal couplers. Because the loading spectra is not presented as a function of train speed, accounting for the mean stress is largely a

matter of conjecture. As such, fatigue cases were calculated using a zero mean stress, and a mean stress at a train speed of 45 mph for a single locomotive for the first drawbar. Although this does not rigorously account for the mean stress, the calculations do provide at least a quailitative measure of the effect.

CONCLUSIONS

- The insertion of a properly sized and installed head brace results in a significant (about 15 to 20 percent) reduction of longitudinal coupler loads and a dramatic (over 75 percent) reduction in vertical coupler loads.
- The fatigue life estimation procedure does not account for the possibility of vibratory impact stresses which may contribute a significant portion of the fatigue damage.
- The GATX type tank car would show a significant decrease in stress at the fatigue critical pad-to-tank weld by increasing the size of the pad.
- Since ACF tank cars were not involved in any leaking incidents, and all 1300 cars in the fleet have been inspected and repaired, this type of car is not considered critical.

RECOMMENDATIONS

- Field testing should be performed to characterize the vibration induced stresses in the reinforcement pad due to yard impact couplings.
- Laboratory testing should be performed to characterize the crack growth properties of the reinforcement pad steel.
- The crack growth of a machined flaw at the weld toe should be monitored during service and correlated with remote strain measurements during the same period. The Simuloader at TTC may be useful for this purpose.

REFERENCES

1. Meacham, H. C., and Ahlbeck, D. R., "A Computer Study of Dynamic Loads Caused by Vehicle-Track Interaction", Trans. ASME, J. of Engineering for Industry, **91**, Series B, (3) 808-816 (August 1969).

2. Martin, G. C., and Tse, Y. H., "Parametric Studies on a Railroad Freight Car Mathematical Model", ASME Paper No. 74-WA/RT-11 (December 1976).

3. Willis, T., "Nonlinear Analysis of Rail Vehicle Dynamics", Sound and Vibration Digest, **8** (10) 19-35 (October 1976).

4. Hussain, S.M.A., Garg, V. K., and Singh, S. P., "Harmonic Roll Response of a Railroad Freight Car", ASME Paper No. 80-RT-2 (April 1980).

5. Henderson, K. A., and Johnson, J., "A Criterion for the Control of 100 Ton Hopper Car Roll Motions", ASME Technical Paper (CN reproduction) (March 27, 1968).

6. Monselle, D., "Truck-Bolster Dynamic Loadings Measured Under Harmonic Roll Conditions", ASME Paper No. 71-WA/RT-6 (December 1972).

7. Martin, A. E., and Smith, L. W., "Determination of Car Body Center Plate Fatigue Design Critieria by Full-Scale Car Testing", ASME Paper No. 74-RT-8 (April 1974).

8. Johnson, M. R., "Summarization and Comparison of Freight Car Truck Load Data", ASME Paper No. 77-WA/RT-3 (December 1977).

9. Johnson, M. R., Evans, R. A., and Guins, S., "Hopper vs. Tank Car Truck Loads", Report No. FRA/TTC-82/03 (November 7, 1981).

10. The Car and Locomotive Cyclopedia, Simmons-Boardman (1981).

11. Powers, R. G., and Stephenson, J. G., "Trainaction Measurements in the Tropicana Univ Train", ASME Paper No. 73-WA/RT-9 (December 1973).

12. Johnson, M. R., Welch, R. E., and Ojdrovich, G., "Analaysis of Truck Bolster Center Plate Rim Response to Impact Loads", ASME Paper No. 74-RT-5 (April 1974).

13. Ahlbeck, D. R., and Doyle, G. R., "Study to Define the Shock and Vibration Environment During Railroad Transport of Shipping Containers", Battelle Report to E.I. du Pont de Neumours and Company, Inc. (August 8, 1974).

14. Magnuson, C. F., and Wilson, L. T., "Shock and Vibration Environments for Shipping Containers on Railcars and Trucks", SAND75-0427, Sandia Laboratories, Albuquerque, New Mexico (June 1977).

15. Petry, S. F., "Rail Tiedown Tests With Heavy Casks for Radioactive Shipments", E. I. du Pont de Nemours & Co., Savannah River Laboratory Report No. D)-1536, (August 1980).

16. Sharma, V., "Coupler Load Environments and Corresponding Fatigue Life Estimates", Association of American Railroads, Report WP-123 (July 25, 1986).

17. Fitzgerald, B. J., Hayes, D., Moustakakis, B., "Evaluation of the Draft 8.11 to Tank Interface", Richmond Tank Car Company Report (May 1987).

18. Pryzybylinski, P., and Halcomb, S., "Interium AAR Guidelines for Fatigue Analysis of Freight Cars", AAR Report No. R-245 (May 1977).

19. Neuber, H., J. Applied Mech., 8 544-550 (December 1961).

20. Peterson. R. E., in Metal Fatigue, Sines and Wais, Eds., McGraw-Hill, New York, Chapter 13 (1959).

21. Coffin, L. F., "Fatigue at High Temperature--Prediction and Interpretation", Proc. Institution of Mech. Eng'rs., 188, 109-127 (September 1974).

22. Morrow, J., Internal Friction, Damping, and Cyclic Plasticity, ASTM STP 378, American Society for Testing and Materials, 45-87 (1965).

23. Tanka, K., Nishijima, S., Mat Svoka, S., Abe, T., and Konzu, F., "Low- and High-Cycle Fatigue Properties of Various Steels Specified in J15 for Machine Structural Use", Fatigue Fract. Eng Mater Strut, 4, 970108 (1981).

24. McMahon, J. C., and Lawrence, F. V., "Predicting Fatigue Properties Through Hardness Measurements", FCP Report No. 105, University of Illinois at Urbana-Champaign (1984).

25. Morrow, JoDean, "Internal Friction, Damping and Cyclic Plasticity", ASTM STP 378, 45-87 (1965).

26. "Evaluation of New Steels for Tank Cars", AAR Report RA-03-7-53 (Draft) (April 29, 1987).

27. "Investigation Into the Cause of Cracking in Railroad Tank Car NATX 34081", Report by Materials Analysis, Inc., Dallas, for GE Railcar Services Corporation (November 12, 1984).

28. "Leakage of Sulphuric Acid at Mileage 173.2, Newcastle Subdivision, in CN Campbellton Yard, Campbellton, in the Province of New Brunswick on January 4, 1986", Canadian Transport Commission Report (January 28, 1987).

29. DOT-105/111/112/114 Tank Cars Shell Cracking and Structural Integrity Assessment, Task Force Report, DOT, Transportation Systems Center, Cambridge, Massachusetts (November 1986).

30. Rolfe, S. T., and Barsom, J. M., "Fracture and Fatigue Control in Structures, Application of Fracture Mechanics", Prentice-Hall (1977).

31. Rooke, D. P., Cartwright, D. J., Compendium of Stress Intensity Factors, The Hillingdon Press, 1976.

32. Lawrence, F. V., Mattos, R. J., Higashida, Y., and Burk, J. D., "Estimation of Fatigue Initiation of Welds", ASTM STP 684, pp. 134-158 (1978).

33. Chang, S. T., Lawrence, F. V., "Improvement of Weld Fatigue Resistance", University of Illinois, FCP Report No. 46 (January 1983).

APPENDIX A

SYNOPSIS OF PERTINENT REFERENCES REGARDING THE LOAD ENVIRONMENT ON 100 TON CARS

Reference 4 (1980)

Pullman Standard/AAR computer simulations of car rocking--100 ton car

Centerplate load -- 128 to 155 kips
Side bearing load -- 111 to 165 kips
Critical speed (14-16 mph)

Reference 5 (1968)

CN tests (Henderson, Johnson) car 100 ton covered hopper car

Side frame lateral -- 45 kips max.
Side frame vertical -- 80 kips dynamic (above 60 kips static reference)
Roll @ 18.3 mph -- 8.10° peak to peak ...for 2-1/2 in. (D3) springs, 3/4 in. cross level error on 39 ft. rail lengths.

Reference 6 (1971)

AAR tests (Monselle) on 100 ton covered hopper car -- 2-1/2 in. (D3) springs, 1/4 in. side bearing clearance, no supplemental snubbing

Roll @ 16 mph	-- 7.3° peak to peak
Centerplate-vertical	-- 140 kips
Side bearing vertical	-- 135 kips
Side frame vertical	-- 88 kips peak (60 kips static)
Side frame lateral	-- 19 kips
On curved track...	
Centerplate vertical	-- 170 kips
Side bearing vertical	-- 158 kips
Side frame vertical	-- 110 kips (~ 70 kips static)
Side frame lateral	-- 20 kips

APPENDIX A

SYNOPSIS OF PERTINENT REFERENCES REGARDING THE LOAD ENVIRONMENT ON 100 TON CARS

VERTICAL/LATERAL LOADS

Reference 1 (1965-1969)

Battelle computer simulations of car rocking on staggered-joint track: (120 kips vertical load on centerplate) Centerplate edge force -- 130 to 160 kips. Side bearing force -- 80 to 150 kips depending on speed, track geometry, snubbing, side bearing clearance, etc. Speeds in 15-19 mph range.

Reference 2 (1975)

AAR computer simulations for different spring groups--

Spring	Centerplate Max. Load, kips	Side Bearing Max. Load, kips
D3	167	157
D5	179	160
D7	157	186

Reference 3 (1976)

T. Willis (IITRI) computer simulation

	IIT Model	Stucki Model
Car size, tons	70	100
Critical speed, mph	17.5	17.5
Peak roll angle, deg.	6.0	6.5
Centerplate vertical reaction, kips	110	170
Wheel vertical load, kips	60	75
Bolster lateral reaction, kips	42	40

Reference 7 (1974)

Dresser (Martin, Smith) tests on 100 ton hopper car

Roll angle @ 16 mph	--	8.8° peak to peak
Side bearing vertical	--	111 kips max.
	--	62 kips average peak
Roll angle @ 16 mph	--	10.9. peak to peak
Side Bearing vertical	--	114 kips max.
	--	71 kips average peak

Reference 8 (1977)

IITRI (Johnson) tests on 100 ton test cars over revenue track

- 100 ton hopper car, D5 (3-11/16 in.) springs
- 100 ton tank car, D3 (2-1/2 in.) springs

Side frame vertical load spectra in load exceedance level per mile; variations in spectra with speed, track quality, car (spring group) type. Most severe with tank car in higher-speed (45-60 mph) in the bounce mode on BJR track. D3 springs tend to go solid in severe bounce. For 60-kips static load level on side frames.

Envelope of Side Frame Load Spectra

Exceedances per Mile	100 Ton Coal Hopper Car (all Speeds)	100 Ton Stone Hopper Car (Good Track all Speeds)	100 Ton Tank Car 15-45 mph	100 Ton Tank Car 45-60 mph
	Maximum/Minimum Load, kips			
100	70/50	66/54	70/50	70/50
10	85/37	73/48	78/42	95/30
1	96/29	79/44	90/35	165/10
0.1	111/24	85/40	110/25	205/0
0.01	116/18	98/36?	150/10?	?
0.001	122/15	?	?	?

Envelope of Side Bearing Load Spectra

Exceedances per mile	100 Ton Coal Hopper Car (15-30 mph)	(30-45 mph)	100 Ton Tank Car 15-30 mph	30-45 mph	45-60 mph
	Maximum Load, kips				
100	51	10	0	0	0
10	80	45	7	5	0
1	100	71	32	25	25
0.1	115	90	52	60	70
0.01	130	110	68	89	>120?

Truck Total Bounce Spectra

		Maximum Measured Loads, kips	Exceedances per Mile
30-45 mph	Coal Hopper Car	210	0.003
	Stone Hopper Car, Good Track	150	0.06
	Tank Car	240	0.018
45-60 mph	Coal Hopper Car	225	0.01
	Stone Hopper Car, Good Track	165	0.04
	Tank Car	360	0.25

Reference 9 (1982)

IITRI/RPI/AAR (Johnson, Evans, Guins) tests of 100 ton hopper and tank cars at FAST vs. revenue track.

Hopper car over railroad test track (RTT) car rocking (shimmed) test section, 20 mph

D5 Springs
- Side frame loads = ± 33 kips maximum dynamic
- Side bearing loads = 70 kips peak

D3 Springs
- Side frame loads = ± 38 kips maximum dynamic
- Side bearing loads = 95 kips peak

Truck Bounce Load Spectra

(D3 Springs)

Exceedance per Mile	Good Revenue Track & FAST, 30-45 mph	Normal Revenue Track 45-60 mph
	Maximum/Minimum Loads, kips	
100	+15/-15	+16/-18
10	+22/-21	+32/-31
1	+31/-25	+47/-42
0.1	+41/-32	+61/-51
0.01	+53/-39?	?

Tank Car Bounce Load Spectra

Exceedance per Mile	FAST, 35 mph	FAST, 45 mph
	Maximum/Minimum Loads, kips	
100	+7/.9	+8/-10
10	+13/-13	+17/-17
1	+19/-17	+27/-24
0.1	+25/-22	+37/-30
0.01	+31/-27?	+49/-34?

LONGITUDINAL LOADS

Reference 10 (1984)

Car & Locomotive Encyclopedia
Maximum starting tractive effort estimated to be 120,000 lb/unit, 80,000 lb/unit at Notch 8, 15 mph. Three units @ 15 mph, maximum tractive effort = 240,000 lb. on first drawbar (draft).

Reference 11 (1973)

Freightmaster (Powers, Stephenson) tests of Tropicana unit train end-of-car (EOC) hydraulic cushioning units. For 1200-mile trip, three events ≥ 300 kips run-out (draft) with maximum event of 380 kips, 6 events ≥ 300 kips run-in (buff) with maximum event -520 kips. There were 480 run-out events on tests with 10 instrumented couplers (Bradenton to Washington D.C.). maximum run-out of 280 kips at cars 42-52; 95th percentile = 190 kips, average of all peaks = 100 kips. There were 10 run-in events ≥ 200 kips for the 57-car train.

Cause of Longitudinal Loading	Maximum Load, kips	Site of Maximum Load Car No.	95th Percentile Load, kips	Average Load, kips
Terrain-induced	-256	22	110	30
Dynamic brake	-350	52		
Air brake	-430	22, 47		

Longitudinal tests on a phosphate train (70 and 100 ton cars, conventional draft gear) produced the following results:

	Run-in Loads, kips		Run-out Loads, kips	
100 T Cars Car No.	Maximum	95th Percentile	Maximum	95th Percentile
1	-250	140	270	167
5	-265	122	345	202
10	-335	185	340	228
15	-400	202	290	212

157 loads (15,626 tons gross weight)
297 events in 225-mile trip
20 events ≥ 200 kips (one or more of the four instrumented couplers showed loads ≥ 200 kips)

Reference 12 (1974)

IITRI (Johnson, Welch, Ojdrovich) tests on bolster response to impact loading-empty 100 ton hopper car ("hammer") hitting three loaded cars ("anvil") with brakes on, track skates behind one wheel of each car.

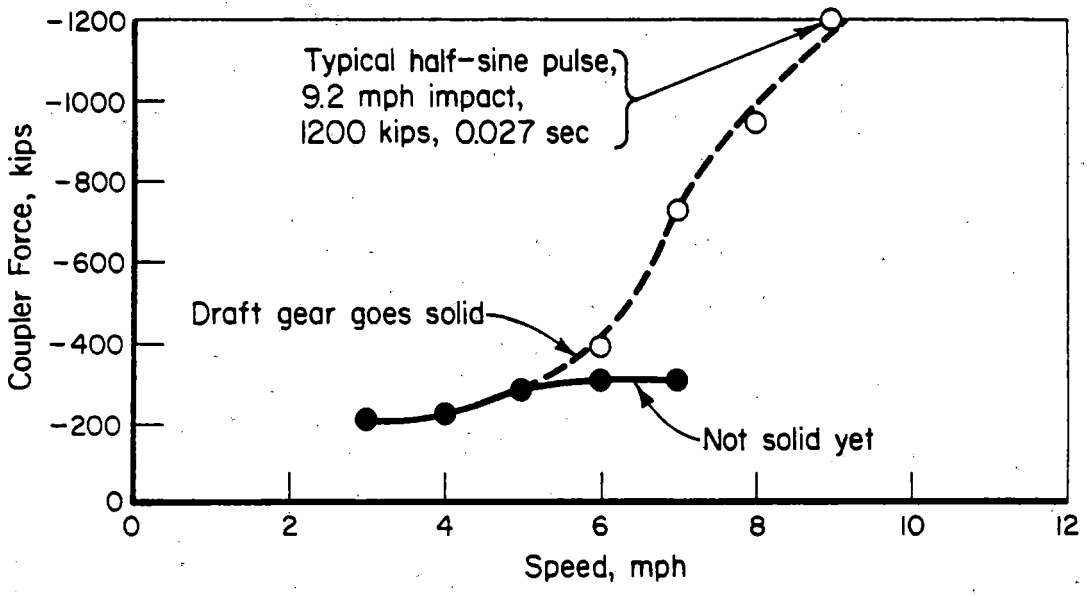

Reference 13 (1974)

Battelle survey for du Pont, yard coupling impacts --

Speed (mph)	Percentage of Events
<6	70
6-7	17
7-8	7
8-9	3
9-10	2
>10	1

Reference 15 (1980)

du Pont impact tests (Petry) at Savannah River Lab. Seaboard Coast Line (SCL) bulkhead, 70 ton flat cars with different-sized casks. Four "anvil" cars loaded with ballast, brakes set, slack bunched.

Cask Weight Tons	Coupler	Impact Speed (mph)	Coupler Force, kips
40	Standard	10.5	-1,160
40	Standard	10.8	-1,210
40	Standard	10.7	-1,220
70	Standard	11.2	-1,620
40	EOC	11.1	-490
40	Cushion UF	10.7	-310

The loads measured were basically 60 millisecond half-sine pulses, followed by a second half-sine of about half the amplitude, and shorter in duration. Related to the above results, the Sandia Labs study[14] showed 99.8 percent of all coupling impacts occur at less than or equal to 11 mph.

Reference 16 (1986)

AAR (Sharma) tests under FEEST program

Longitudinal Load (Exceedance) (Kips)	No. of Occurrences Loaded 100 Ton Hopper* Buff	Draft	No. of Occurrences Empty 100 Ton Hopper** Buff	Drafts
500	1	-	3***	-
480	-	-	4***	-
460	1	-	-	-
440	1	-	-	-
420	-	-	-	-
400	2	-	-	-
380	18	-	-	-
360	61	-	-	-
340	82	1	-	-
320	64	20	-	-
300	91	42	4	-
280	165	36	3	-
260	155	65	6	-
240	245	105	6	2
220	520	275	8	1
200	1100	605	12	1

* Traffic Makeup:
"Severe" Unit Train -- 5625 Miles
"Normal" Unit Train -- 8414 Miles
General Service -- 748 Miles
14787 Total Miles

** Traffic Makeup:
Unit Train -- 6037 Miles
General Service -- 791 Miles
6828 Total Miles

*** Yard Impact Load